

Re-Design and Testing of the WPI Kite Power System

A Major Qualifying Project Report
submitted to the Faculty
of the

WORCESTER POLYTECHNIC INSTITUTE

In partial fulfillment of the requirements for the
Degree of Bachelor of Science
In Aerospace Engineering

SUBMITTED BY:

Adam Cartier
acartier@wpi.edu

Eric Murphy
emurphy@wpi.edu

Travis Perullo
tperullo@wpi.edu

Matthew Tomasko
tomasko@wpi.edu

Kimberly White
kjl1118@wpi.edu

Professor David Olinger, Project Advisor

1. Abstract

The goal of this project was to upgrade and modify the current WPI kite power system that has been in development over the past several years. Kite power has a potential to improve upon current wind turbine technology by allowing access to higher wind velocities at large altitudes, while reducing environmental impact. The system developed by previous MQP teams is based on a large kite tethered to a rocking beam that is 5 meters in length, which turns a gear train and generator. Modifications to this system in the current project include; use of more stable, larger sled kites, an upgraded gear shaft, a new mechanism to change the kite angle of attack and refined data acquisition tools including the capability to measure kite tether tensions during field and lab testing. These refinements were thoroughly tested in both the field and the lab. In the lab testing known loads were applied to the rocking arm end for the first time during dynamic tests. Wind tunnel tests on rigid, scale-model sled and delta kite shapes were also conducted to measure aerodynamic coefficients. In the field, sled kites were used for the first time and found to stall and return to original altitude in a controlled manner when trailing edge lines were added. When the entire system was brought to the field, the tests showed our sled kites would create enough force to lift the rocker arm, generating power.

2. Table of Contents

1. Abstract	2
2. Table of Contents	3
3. Table of Figures	4
4. Introduction	6
5. Background	11
6. Previous Work by WPI Project Teams	18
7. Project Objectives	20
8. System Mechanical Improvements	21
Safety Brace	21
Rear Belt System	23
Stall System Improvements	24
9. Instrumentation	27
Load Cell	27
Power Source	29
LabVIEW	29
10. Lab Testing	33
Wind Tunnel Testing of Model Kites	36
11. Field Testing	42
12. Conclusions	51
13. Future Work	53
14. Reference List	55
15. Appendix	56

3. Table of Figures

Figure 1: Atmospheric Carbon Dioxide (Elmherst 2003).....	7
Figure 2: Wind Power, Top Ten Countries	8
Figure 3: Wind Power, Existing World Capacity	8
Figure 4: Power Output and Wind Velocity for Turbine and Kite area of 10m ² (Buckley, 2008)..	10
Figure 5: Goela Kite Models (Goela from Reference 7)	14
Figure 6: Conyne Kite Model (Goela from Reference 7)	15
Figure 7: Goela Spring Mechanism View 1, (Goela from Reference 7)	15
Figure 8: Goela Spring Mechanism View 2 (Goela from Reference 7)	16
Figure 9: Kite Gen Schematic (Kite Gen 2005).....	16
Figure 10: Highest Wind System (Reference 10)	17
Figure 11: WPI Kite Power System (Buckley 2008).....	19
Figure 12: Previous Locking Mechanism	21
Figure 13: Profile View of New Locking Mechanism.....	22
Figure 14: New Locking Mechanism	23
Figure 15: Previous Kite-Stall Mechanism.....	25
Figure 16: New Kite-Stall Mechanism	26
Figure 17: 2008-2009 MQP Load Cell Design	27
Figure 18: Load Cell Apparatus	28
Figure 19: Calibration of Final Load Cell Apparatus.....	28
Figure 20: 2008-2009 LabVIEW	30
Figure 21: 2009-2010 LabVIEW Update	31
Figure 22: 2009-2010 LabVIEW Block Diagram	32
Figure 23: Kite System Testing Using Sandbags to Simulate Kite Tension.....	33
Figure 24: Lab Test-Kite System Weight Drop	35
Figure 25: SolidWorks Model Delta Kite	36
Figure 26: SolidWorks Model Sled Kite	36
Figure 27: Sled Kite Lift Coefficient.....	38
Figure 28: Drag Coefficient of Sled Kite	38
Figure 29: Delta Kite Lift Coefficient	38
Figure 30: Drag Coefficient of Delta Wing.....	39
Figure 31: Lift and Drag Coefficient of Sled Kite.....	39
Figure 32: Lift, Drag, and Tension for Sled Kite at 1 Degree AOA	40
Figure 33: Power Sled 14 (http://www.premierkites.com/collections/pdf/Sleds.pdf).....	42
Figure 34: Jumbo Power Sled 36 (http://www.premierkites.com/collections/pdf/Sleds.pdf)	43
Figure 35: Mega Power Sled 81 (http://www.premierkites.com/collections/pdf/Sleds.pdf)	43
Figure 36: Kite Stalling Mechanism.....	44
Figure 37: Stall of PowerSled 36	45
Figure 38: Stall of PowerSled 81	46
Figure 39: Full System Test with Kite	47
Figure 40: Overview of System	48
Figure 41: Full Data Set from Kite System Test	49

Figure 42: Kite Stalls from Kite System Test	49
Figure 43: Test One without Flywheel	56
Figure 44: Test Two without Flywheel	56
Figure 45: Test One with Sliding Mechanism	57
Figure 46: Test Two with Sliding Mechanism	57

4. Introduction

As population increases there is a greater demand for sources of clean, economical, renewable sources of energy to replace the dwindling supply of non-renewable resources. The high cost of fossil fuels, along with climate change concerns has stimulated investment, research into power production, and mandates relating to renewable energy. While a full transition to renewable energy is years away, the latter half of this decade has shown dramatic growth in many indicators of renewable energy alternatives even in the face of the 2009 economic crisis. The renewable energy market grew very rapidly in 2008, and among these new renewables, wind power was the second largest addition- besides large hydropower¹.

Wind power is the conversion of wind energy into a more useful form such as electrical or mechanical energy. Society has harnessed the wind for thousands of years using sailboats and ships, and for hundreds of years as a source of mechanical energy from windmills. More recently large-scale wind farms use wind turbines to convert the kinetic energy of the wind into electrical power, allowing transmission to the energy grid without byproducts that pollute the environment. Nearly one hundred percent of the world's wind power is currently produced using wind turbines². This form of renewable energy is becoming more popular, with a global 29 % increase in capacity to 121 gigawatts in 2008¹. Figures 1 and 2 show the existing world capacity of wind power, as well as the distribution of that capacity among the top ten countries in 2008. In 2008, the United States overtook Germany as the leader in wind power capacity.

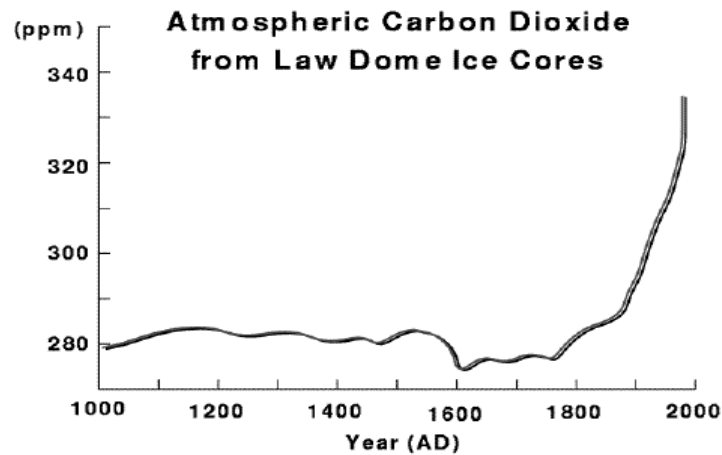


Figure 1: Atmospheric Carbon Dioxide (Elmherst 2003)

As human reliance on energy grows, so do the carbon dioxide levels in our atmosphere, a result of the leading methods in which we obtain our energy presently. CO₂ levels have increased rapidly since 1800--the start of the industrial revolution when fossil fuels were first used extensively-- to unprecedented levels in the last 400 thousand years. This rise in Carbon Dioxide levels has been linked to cause of global warming—the absorption of infrared radiation by the earth’s atmosphere containing this gas. Figure 1 shows how atmospheric carbon dioxide has increased in the past 1000 years, with a dramatic increase starting around 1800.

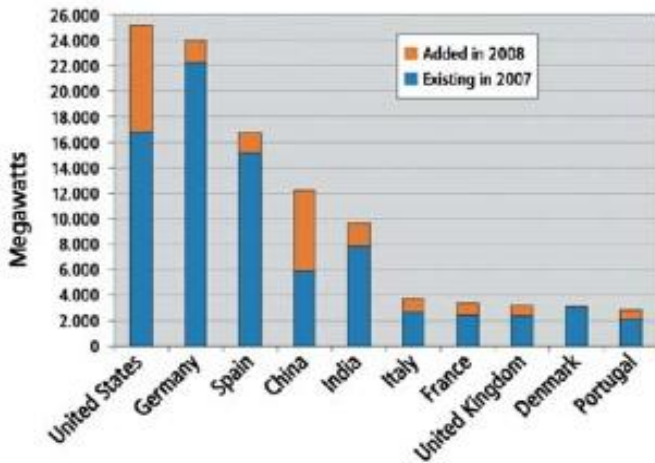


Figure 3: Wind Power, Existing World Capacity (Reference 1)

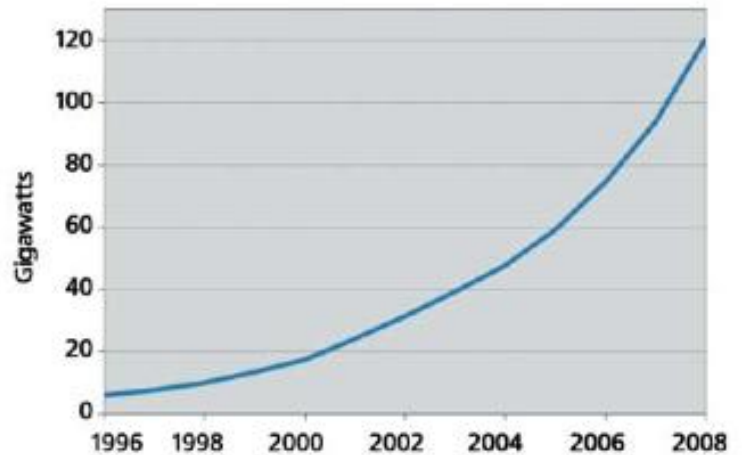


Figure 2: Wind Power, Top Ten Countries (Reference 1)

In the search for alternative clean energy, wind power is a popular alternative.

Figures 2 and 3 show the growth of wind power capacity in the world from 2007-2008 and since 1996 in the top ten countries, respectfully. The dominant method of capturing this energy, the wind turbine, has many disadvantages. Wind turbine performance is based upon the size and height of the turbine blades. While increasing the size and height of turbine blades, construction of substantial support structures are required to bear the load of the generator and blades increased size, which incurs large expenses. Another such disadvantage is the noise pollution they create. In concert with one another, large wind turbines can create profound noises, comparable to jet engines on a runway, which extend out for more than a mile (WVMCRE website). Another disadvantage is finding an appropriate location for a wind farm. In order to make their implementation cost effective and more efficient, wind turbines are used in vast numbers on wind farms in strategic places. The disadvantage with vast wind farms is wind turbines are generally described as aesthetically displeasing in design, which makes them unwelcome near most areas. Wind farm placement becomes more difficult with the intermittency of the source of the energy,

wind. Areas that require a high amount of energy are generally not in a prime area for wind farms, thus these areas are forced to rely on other means of energy. On the other hand, areas that require minimal energy, described as “off the grid,” are not fiscally able to justify the use of an expensive, large wind turbine.

Recent studies into different options of generating wind power have resulted in a resourceful solution, using kites. These kites can be cheaply built and transported to areas at a lower cost where it is not feasible to capture wind energy with turbines. The greatest improvement over wind turbines is the performance potential of kites at higher altitudes. At higher altitudes wind velocities are higher making power generation likewise consistent and reliable. Equation (1) shows that wind speed increases following a 1/7th power law where V is velocity and y is the height, while the subscript 0 denotes a reference condition.

$$V = V_0 \left(\frac{y}{y_0} \right)^{1/7} \tag{1}$$

Given that power increases proportionally to the cube of wind speed, a kite at a higher altitude will have greater power potential. Figure 4 shows how altitude effects wind speed and power as well as the range of altitudes that turbines and kites can successfully operate in. The potential of the kite power system coupled with lower costs, quiet operation, easy transportation and minimal special requirements make this energy alternative a practical solution for developing countries or areas far off the power grid.

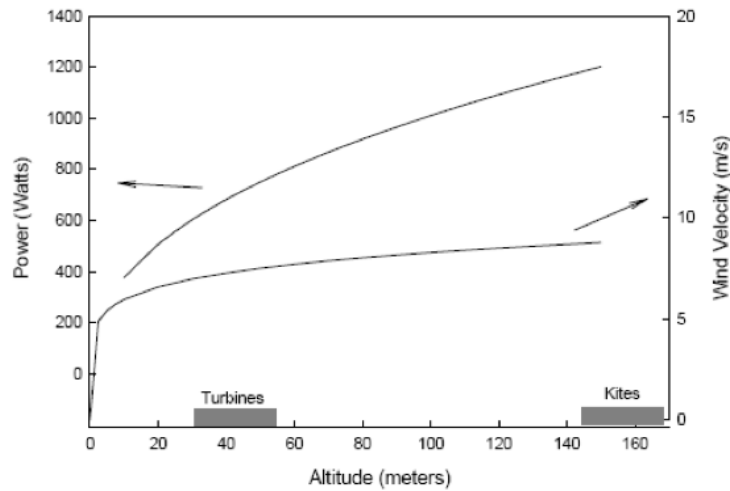


Figure 4: Power Output and Wind Velocity for Turbine and Kite area of 10m² (Buckley, 2008)

The goal of this project was to upgrade and modify the current WPI kite power system that has been in development over the past several years. The system developed by previous MQP teams is based on a large kite tethered to a rocking beam that is 5 meters in length, which turns a gear train and generator. As the kite rises, one side of the beam moves upwards pulling a tether and turning the generator, which in turn produces power. At the top of the beam's movement, a sliding mechanism moves backwards on its track due to gravity and pulls on the trailing edge of the kite, effectively stalling it. There is a reduction of force on the beam as a result of the kite stalling and thus the beam falls. As the other end of the beam rises, a tether is pulled, continuing the motion of the generator. At the bottom of the beam's movement the slider resets to the front of its track, releasing the pull on the trailing edge and allowing the kite to climb again, completing the cycle. Modifications to this system in the current project include; use of more stable, larger sled kites, an upgraded gear shaft, a new mechanism to change the kite angle of attack and refined data acquisition tools including the capability to measure kite tether tensions during field and lab testing.

5. Background

Wind has long been utilized as a source of energy for numerous uses throughout history in the forms of grain and water mills, but the idea of using large kites to capture this energy to generate electrical power has only been considered for a relatively short time.

Some research into the topic began in 1825 by G. Pocock, who had theorized that large kites may be successfully employed to harvest mechanical energy. Pocock began small in his childhood, pulling large rocks and similar objects across the ground with kites, and his work culminated in his invention, the “Charvolant”. The Charvolant was a kite drawn buggy, powered by two kites on lines 1,500-1,800 ft in length, and controlled by large spools mounted on the front of the buggy. At the time horsedrawn buggies were the most common type of transportation, and Pocock’s Charvolants could reach speeds of up to 20 mi/hr, rivaling even the fastest of the horse drawn buggies.³

In 1979, M. L. Loyd began an investigation into the practicality of harvesting wind energy from kites⁴. Loyd developed a governing set of equations that detailed the crosswind kite motion, and applied these equations to modern airfoils. Loyd’s calculations indicated that a 2000m² kite flying at an altitude of 1200m could potentially produce upwards of 45MW of power.

Dr. J.S. Goela also focused on researching and developing kite power solutions in the late 1970s through the 1980s. While at the Institute of Technology at Kanpur, Goela researched the viability of using the motion of a kite to generate power. He also developed his own set of equations to govern the motion of the kite, and used them to predict the ability of a kite to generate power.⁵ In this same publication Goela confirmed a result previously reported by Loyd, that power output would be maximized when the kite moves

in the crosswind direction. Many of Dr. Goela's ideas have been employed in the development of this kite power system, and he has also been involved as a technical consultant to the WPI MQP teams working on the project since its inception in 2007. Goela also carried out some wind tunnel tests of numerous kite models, providing some analysis for the effect of wind loading on kites.⁶ Dr. Goela's published works have lent a great deal of useful information to this project, including an analysis of the steady state of motion of the kite during both its ascent and descent, and from there determined the relative efficiencies of a kite system.⁷

To simplify the analysis of the dynamics of kite motion, Goela broke the cycle of a kite's motion into two parts, ascent and descent. During the initial ascent phase, the kite deployed to accept wind and gain altitude, producing power. During descent, the kite falls back to its original position and work is done on the system. Goela also included that the power coefficient of the system is at its maximum when there is a large lift to drag ratio present. He also indicated that when the kite flies directly against the wind during descent, the power coefficient is at a minimum.⁷

After developing the required mathematical background, Goela and his team turned to practical testing, beginning with examining the performance of different types of kite designs (Figure 5). After rigorously testing numerous kite designs for one that suited the design constraints, a "conyne kite" was selected (Figure 6). Goela chose this particular model for its versatility in the air, commenting "it incorporates the lifting advantage of a flat kite with the stability of a box kite"⁷.

With the kite model selected, Goela turned his attention to the problem of what mechanism will be employed to translate the kite's harvested energy to mechanical energy

on the ground level. Goela's system was designed to hoist a bucket of water over a vertical distance in a well.⁵ Goela's kite power system was comprised of a balanced beam on a fulcrum with spring-loaded assists (Figures 7 and 8).

The springs featured in the system are used to vary the angle of attack of the kite. This occurs as the beam reaches the top of its path, and the water in the bucket is emptied. This action causes the angle of attack to put the kite into a descending trend, allowing the beam to return to its original position and the bucket lowered back into the well. This series of actions is displayed in Figure 8. With the change in angle of attack, the bucket becomes heavier than the tension in the wire and the kite is pulled back down to its initial position. The cycle will begin again when the level is pushed in the opposite direction during the kite's descent. Goela's system was initially intended to lift a bucket full of water out of a well, and so was never integrated into this particular project.

In 2005, an analysis of six different kite powered systems was carried out by David D. Lang. His analysis placed heavy emphasis on factors such as scalability, autonomy, ease of production, and maximum energy capacity. The design labeled KIWI Gen, also known as the Kite Gen design, scored the highest overall in Lang's presentation. While all of the designs had their own merits, they were all rather unfeasible with very low power outputs. The Kite Gen design, on the other hand, has actually been in development for a number of years now.⁸

A project known as the "Kite Wind Generator" or Kite Gen has been in development in Milan, Italy since 2007 and is showing great promise. The goal of the project is to eventually replace nuclear plants completely. The design focuses around a massive rotating structure that is driven by a number of kites tethered to it. As wind causes forces to be

exerted on the kites, the mechanism rotates about a shaft, producing mechanical energy which is then translated into electrical power. The flight path of each kite is controlled by complex avionics software developed for this specific use. This design is estimated to be able to produce as much energy as a nuclear power plant for as little as a thirteenth of the cost per megawatt.⁹ Figure 9 details an illustration of the Kite Gen design.

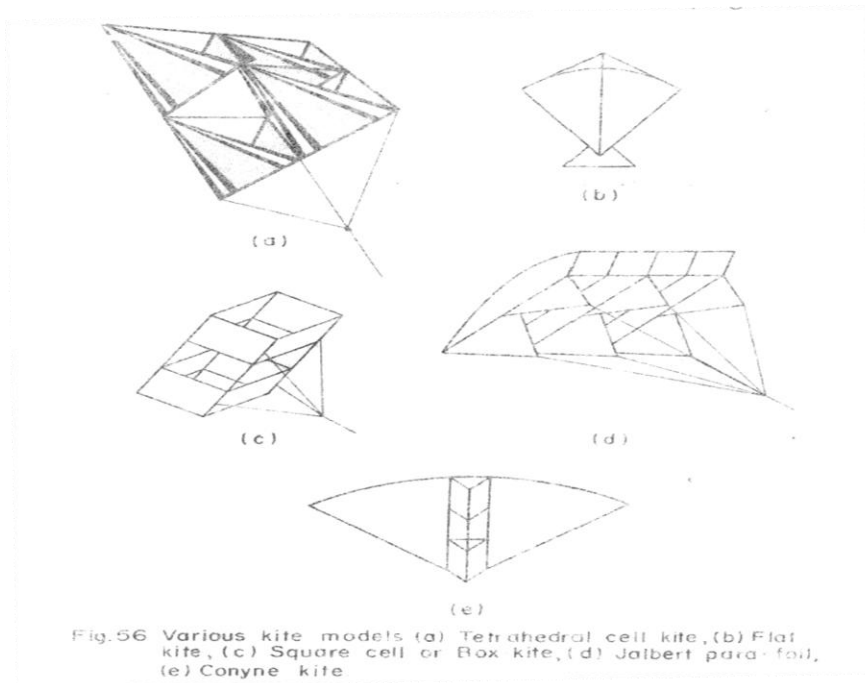


Figure 5: Goela Kite Models (Goela from Reference 7)

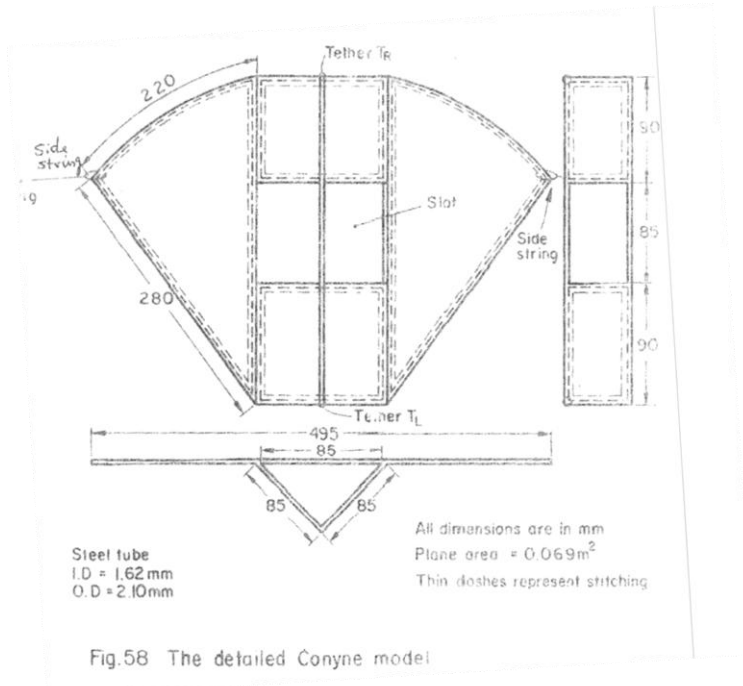


Figure 6: Conyne Kite Model (Goela from Reference 7)

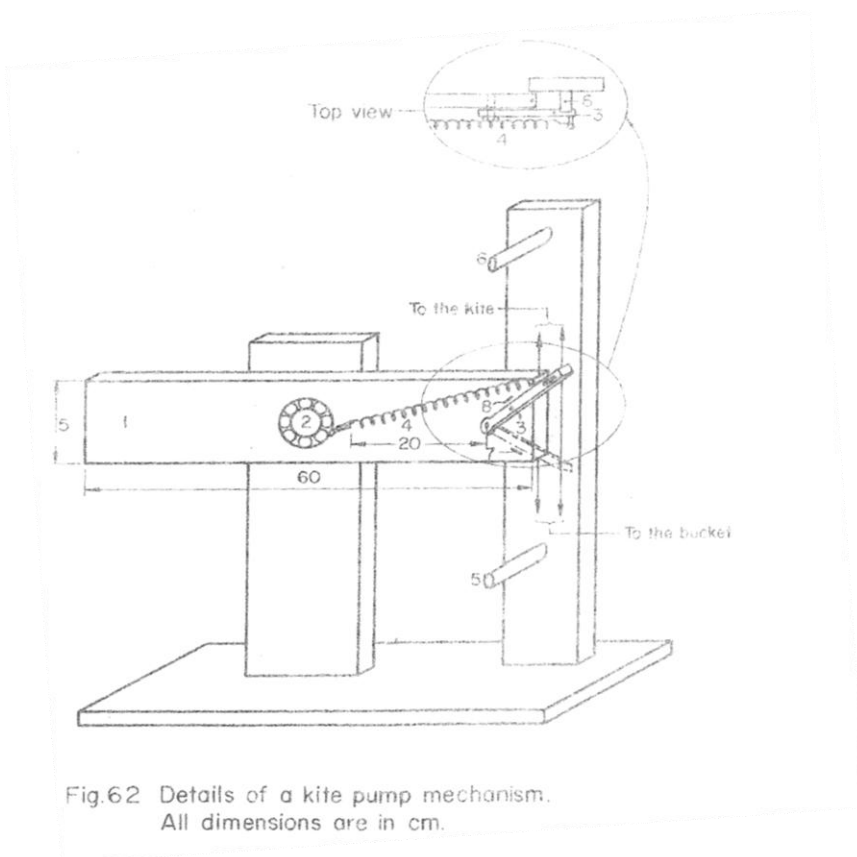


Figure 7: Goela Spring Mechanism View 1, (Goela from Reference 7)

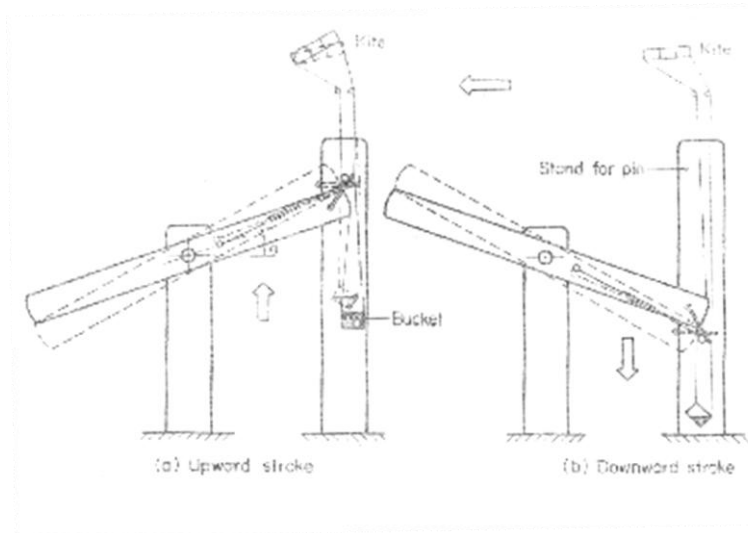


Figure 8: Goela Spring Mechanism View 2 (Goela from Reference 7)

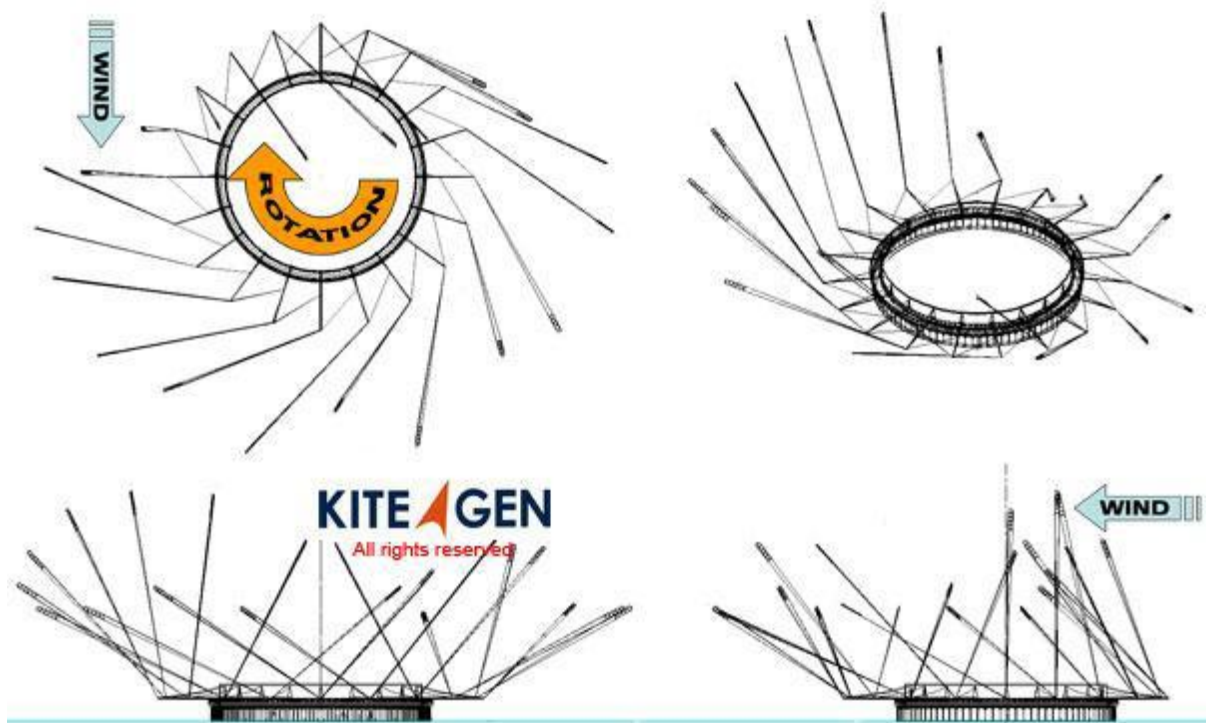


Figure 9: Kite Gen Schematic (Kite Gen 2005)

Highest Wind LLC, a company from Newmarket, New Hampshire, also focuses on harnessing wind power from areas with low wind using their Highest Wind Energy Gliders. Their proposed Energy Glider is 40ftx40ft, weighing 300lbs and flies between 700 and

1200 feet. In order to create electricity, this glider is attached by a high-strength tether to a generator on the ground. As the glider rises, it pulls the line upward with more than a ton of force, then descends allowing the tether to reel itself in. This cycle of rising and descending is repeated every 30 seconds and has the ability to generate 30 kilowatts of power day and night if allowed to run continuously. The figure below shows the system set-up with a power trailer which houses the generator, tether, and sends radio signals to the glider. The glider rests on a stand, shown on the right side of the figure, when wind conditions are poor or system is not in use. Highest Wind LLC plans to begin selling their energy glider system beginning in 2011.¹⁰

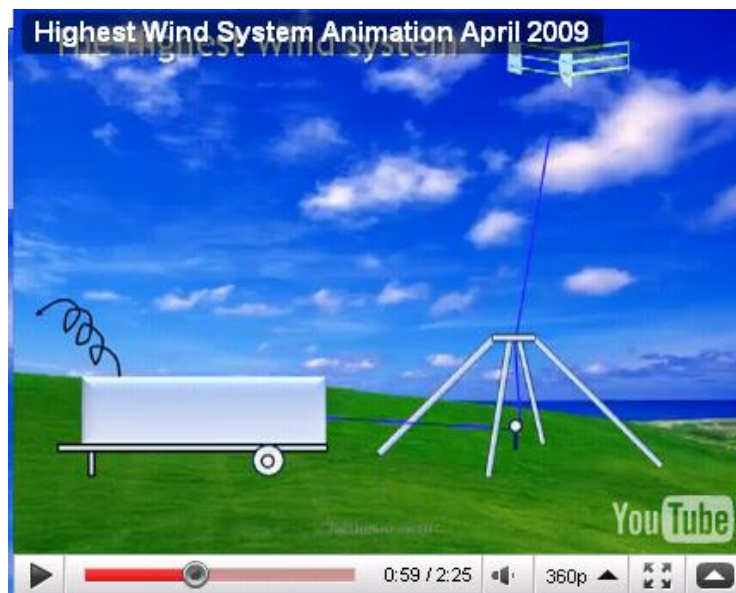


Figure 10: Highest Wind System (Reference 10)

6. Previous Work by WPI Project Teams

Research for this project was greatly supplemented by work done by previous MQPs. In 2006-2007 the team studied numerous different conceptual designs and various kites before designing A-frame and rocking arm assembly that is still in development today. The concept utilized a sliding mechanism on the arm to change the angle of attack of the kite, giving the team the ability to force a stall in the kite, bringing it back down to its initial position without the need for electronic motors. This mechanism was heavily influenced by Goela's bucket design. The team also tested the efficiency and feasibility of numerous different kite styles before deciding on a kiteboarding kite.¹¹

The following year, the project group began the task of fully building the design of the previous project team. The six-foot tall A-frame structure, displayed in Figure 6, serves as the structural core of the system and housing for electronic and mechanical components. A hollow metal rocking arm is mounted at the top of the frame, which is connected to a gear train and sprag-clutch assembly via nylon cords. When the force of the wind pulls the kite up, this force is transferred through the tether line to the rocking arm, which is pulled upward. A nylon tether attached to the end of the rocking arm pulls a sprag clutch, which in turn powers the gear mechanism within the device, and it is this mechanism that is capable of being connected to a battery bank, allowing the mechanical energy created by the kite to be harvested as electrical energy. When the kite reaches the upward position, a sliding mechanism on the bar slides down towards the structure. As the kite is tethered to this slider, when it slides down it stalls the kite, allowing the counterweight to move the rocking arm back into its original position. Once this is achieved, the slider slides back into its original position, allowing the kite to move to a lift producing position once again. This

cyclical motion will allow the structure to harvest wind as long as there is enough to keep the kite afloat.¹²

In the 2008-2009 academic year, another project team took to further improving the system. Their focus included incorporating instrumentation to the system, including an inclinometer to measure the angle of the rocking arm, a force meter to record the force exerted on the rocking arm end, a torquemeter for the gear assembly, and magnetic pick-ups to record the shaft speed of the gear assembly. With all of this instrumentation in place, the mechanics of the kite power system can be accurately interpreted and presented. The team also put a great deal of effort into improving safety precautions regarding the system, as the rocking arm can achieve a dangerous amount of downward force.²



Figure 11: WPI Kite Power System (Buckley 2008)

7. Project Objectives

The goals of this year's project are as follows:

- Thoroughly test our stable, larger sled kites and determine if sled kites can be stalled in a controlled manner by adding two control lines to the kite's trailing edge
- Upgrade the structure's gear shaft
- Create a new, lighter mechanism to stall kite
- Refine data acquisition tools including developing a method to measure kite tether tensions using a load cell.
- Thoroughly test the redesigned WPI kite power system in both the field and lab

8. System Mechanical Improvements

Safety Brace

In order for safe transport, set up, and take down of the system the beam needs to be locked parallel to the ground. In order to accomplish this in previous years a locking device was implemented at the point of rotation, shown below.



Figure 12: Previous Locking Mechanism

The metal used in this device was relatively malleable, as it needed to be bent in house to fabricate. In the process of preparing to test, this device was bent and was no longer able to keep the rocking arm stationary when attached. If the device was bent back to its original form, it would only become easier to bend when a load was applied to it again. With this in mind a new device was fabricated.

In creating a new device to immobilize the arms of the system the following design criteria were considered:

- Reliability and strength

- Ease of attachment/detachment
- Ease of fabrication
- Available materials

Before designing possible new devices, the merits of the original device were considered. While it certainly didn't fail abruptly or catastrophically, it did bend significantly under forces could easily be seen in the field. It was also difficult to attach or detach consistently. Finally, the original design would require relatively precise machining given that the holes on each side need to be in line with each other, which is entirely reliant upon the hinge being attached correctly.

Giving consideration to the drawbacks to the current design, a new device was designed and fabricated from 3in x 5in angle iron, as shown below.

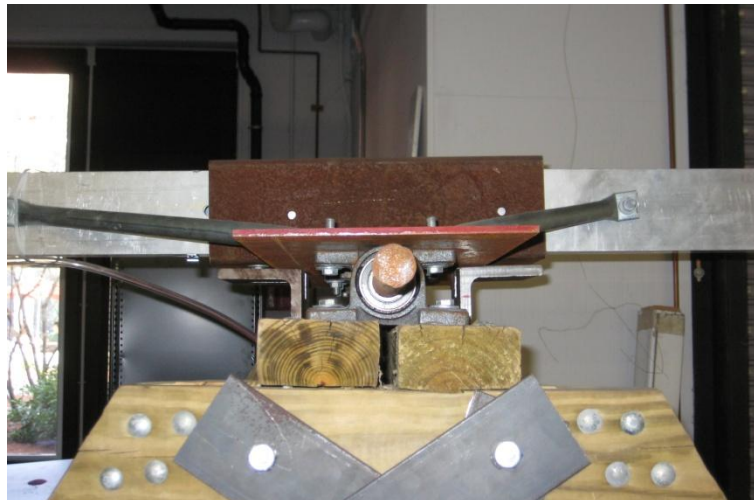


Figure 13: Profile View of New Locking Mechanism



Figure 14: New Locking Mechanism

The new design is attached one half at a time, and in doing so requires less effort. It was also significantly simpler to machine. The angle iron was first cut to length using a horizontal band saw. An end mill was used to make a notch in the middle to accommodate the large bolt located on each arm. A drill press was then used to machine the holes in the angle iron based on the dimensions of the beam it would be attached to. After this, the pieces of angle iron were clamped to the beam, and pilot holes were drilled. Threaded lag bolts were screwed into these pilot holes, finalizing the design. Wing nuts were used to ensure that the angle iron would not fall off of the beams.

Rear Belt System

The rear belt system was added to the frame by the 2008-2009 MQP group and uses a second nylon cord attached to the opposite end of the rocking arm to use the energy of the kite's descent as a secondary power source. The belt system is connected to a metal line that connects to the system's arm by a C ring. The C ring was catching on the PVC pipe which guides the belt/metal line. In order to rectify this problem a PVC funnel was attached

to the pipe, in turn increasing the area which the C ring had to travel through and completely eliminated any catches or snags.



Figure 14: Rear Belt System

Stall System Improvements

Last year's group created a mechanism for stalling a kite-boarding kite based around a slider attached to the end of the beam which the kite is attached to. The mechanism also stabilized the kite-boarding kite, however in doing so added considerable weight to the end of the arm.



Figure 15: Previous Kite-Stall Mechanism

Given that this year's project has centered around sled kites which are significantly more stable than kite-boarding kites, the stabilizing component of the mechanism was rendered obsolete. As a result we were able to remove it, and in turn lowered the weight on the end of the arm considerably. Without the stabilizing mechanism attached to the top of the slider we were able to shorten the slider significantly. This further decreased the weight of the slider and as an added bonus increased the travel of the slider, in turn making it easier stall the sled kite consistently. Finally, the clamps for the trailing edge bar were attached with a spacer that can be removed and replaced with added weight.

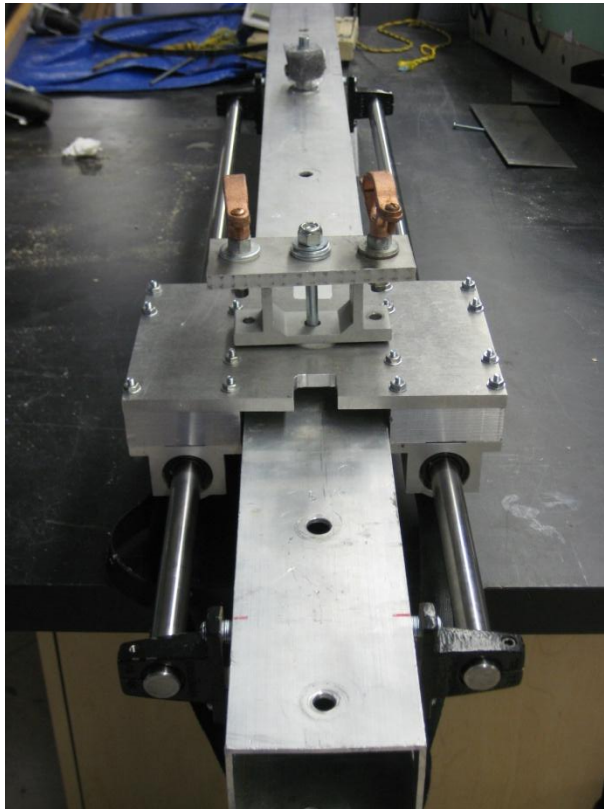


Figure 16: New Kite-Stall Mechanism

The ability to add specific amounts of weight allows the slider to adapt to different sized kites. If a small kite is used there is less lift force, and as a result a heavy slider would not be effective. However if a larger kite is used more force on the trailing edge is required to induce a stall. The new slider design allows for both scenarios and ultimately makes the system more versatile.

9. Instrumentation

In order to determine experimental power, instrumentation and sensors are applied to the kite system. Four sensors are currently connected to a data acquisition system, which reports data regarding the system. There is a load cell to calculate tension in the tether between the system and the kite, an inclinometer to calculate inclination of the rocker arm, torquemeter to measure the torque on the drive shaft, and finally a tachometer to measure the rotations per minute of the drive shaft.

Load Cell

In order to accurately calculate tension in a wire or rope a force meter or load cell must measure tension directly along the axis corresponding to the angle of the kite tether to the rocking arm. The 2008-2009 MQP team developed a system to measure tension perpendicular to the rocking arm.

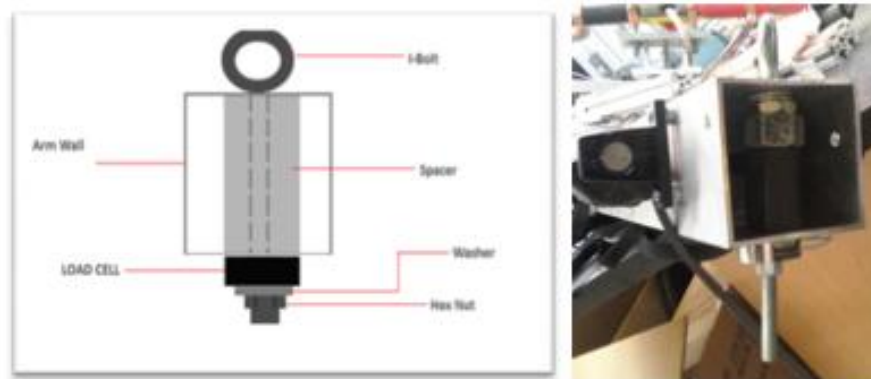


Figure 17: 2008-2009 MQP Load Cell Design

Unfortunately, the kite will not fly directly perpendicular to the rocking arm and therefore the load cell reported inaccurate data. Both the rocking arm and kite tether are in constant motion and the angle between the two will not always be perpendicular. It is

also possible that friction between the eyebolt (Figure 17) and the rocking arm affected the load cell tension measurements.

Therefore the load cell apparatus was redesigned to freely move as the kite tether moves due to wind forces. The design utilizes two eyebolts; one fastens to the rocking arm and the other fastens to the kite tether. Assuming there is always tension in the kite tether, the two eyebolts will be pulled apart and the load cell will always be precisely along the axis of the kite tether. The following figures show the redesigned load cell. The circular load cell is placed within the aluminum block and then compressed between a washer and nut once a force is applied to the kite. The compressive force equals the tensile force from the kite. Figure 19 shows the final load cell apparatus being calibrated by hanging known weights to simulate the kite line forces experienced in the field.

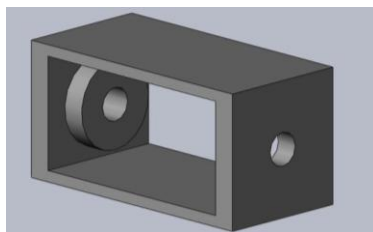


Figure 18: Load Cell Apparatus



Figure 19: Calibration of Final Load Cell Apparatus

Power Source

The data acquisition device developed by the 2008-2009 MQP team required a minimum of 9 watts of power in order to correctly report data from the load cell. In order to generate the power, the team attached two power sources to the data acquisition device, a USB cable and an AC adaptor. This posed problems for testing because there is not always access to an outlet in remote locations.

Therefore we developed a new power source based on two USB cables. A USB cable contains four wires, two for data and two for power. When connected to a powered USB port, such as a laptop computer, the USB cable transmits 5 watts of power. In comparison, the AC adaptor chosen by the 2008-2009 MQP team transmitted 10 watts of power. When running on AC adaptor and USB power, the data acquisition unit received 15 watts of power, but when running on two USB cables the unit only receives 10 watts of power. This is more economical and is above the required 9 watts of power to run the load cell. Not only that but when attached to a laptop, the data acquisition unit becomes more mobile than before which enabled better field-testing results and data acquisition.

LabVIEW

The four sensors convert mechanical properties into voltages, which are transmitted to the data acquisition device and finally to a computer through a USB port. The voltages require conversion from electron volts to their respective units. The 2008-2009 MQP developed a working VI in LabVIEW, which displays force, degrees, torque, and rotations per minute in real time. Not only that, but the data is written to an excel file with a click of the button.

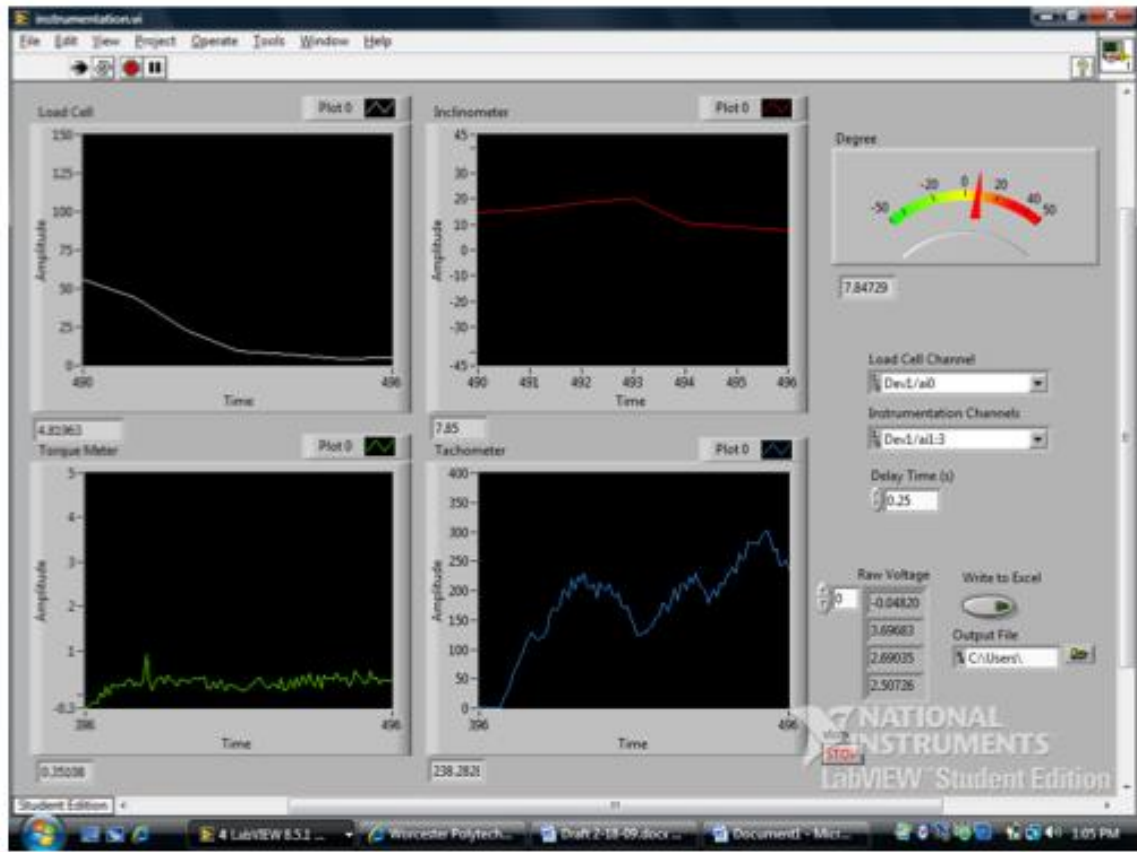


Figure 20: 2008-2009 LabVIEW

Modifications were made to the VI in order to report instantaneous power. Using the rotations per minute and the torque on the drive shaft, an experimental instantaneous power output can be predicted in real time using the following equation:

$$P(t) = \tau(t) \cdot \frac{2\pi \cdot rpm}{60} \tag{2}$$

The updated VI block diagram and graph are in the figure below:

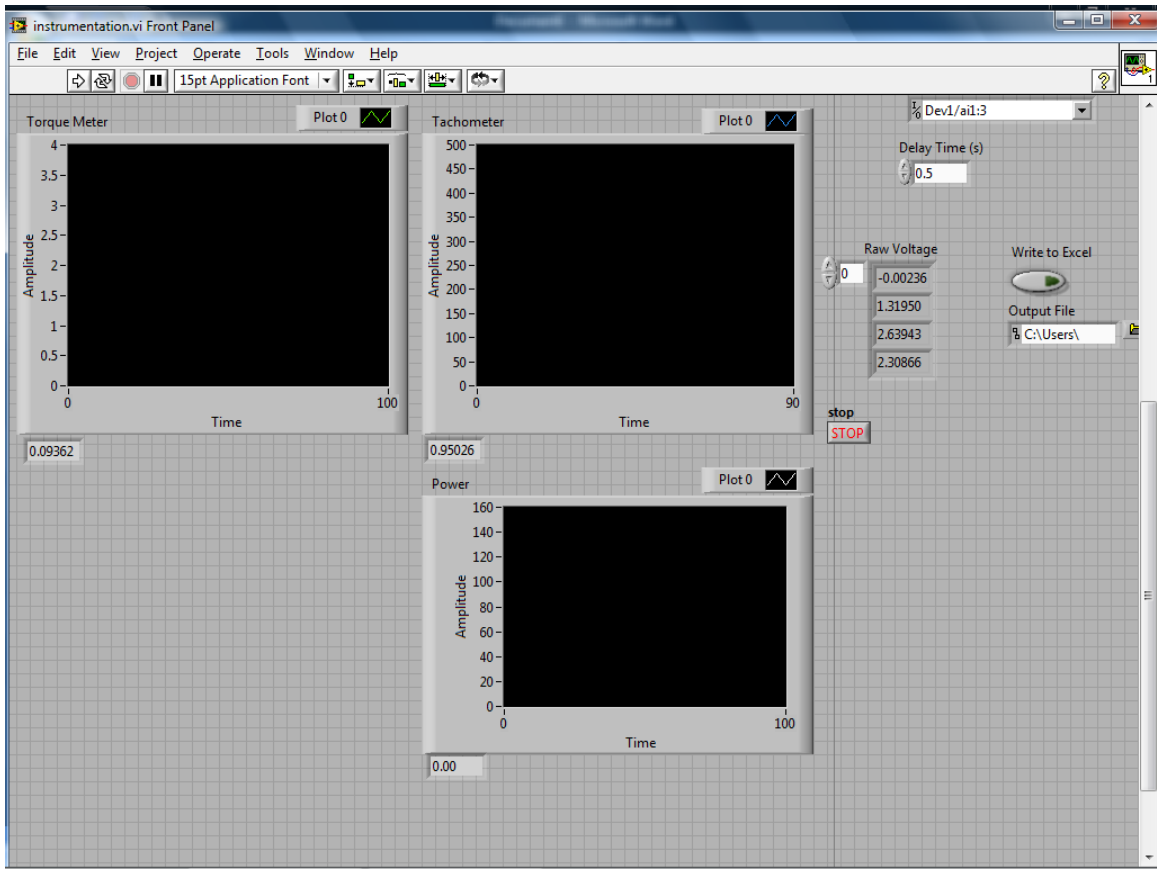


Figure 21: 2009-2010 LabVIEW Update

The plot area at the bottom right of Figure 21 shows the real time power based on the previous equation. This will be beneficial when working in the field to make rapid changes to the kite system based on power results. This plot, coupled with a voltmeter on the generator will fully encompass the power capabilities of the kite system.

Below is the updated block diagram built in LabVIEW that converts the data for the user interface displayed in Figure 22:

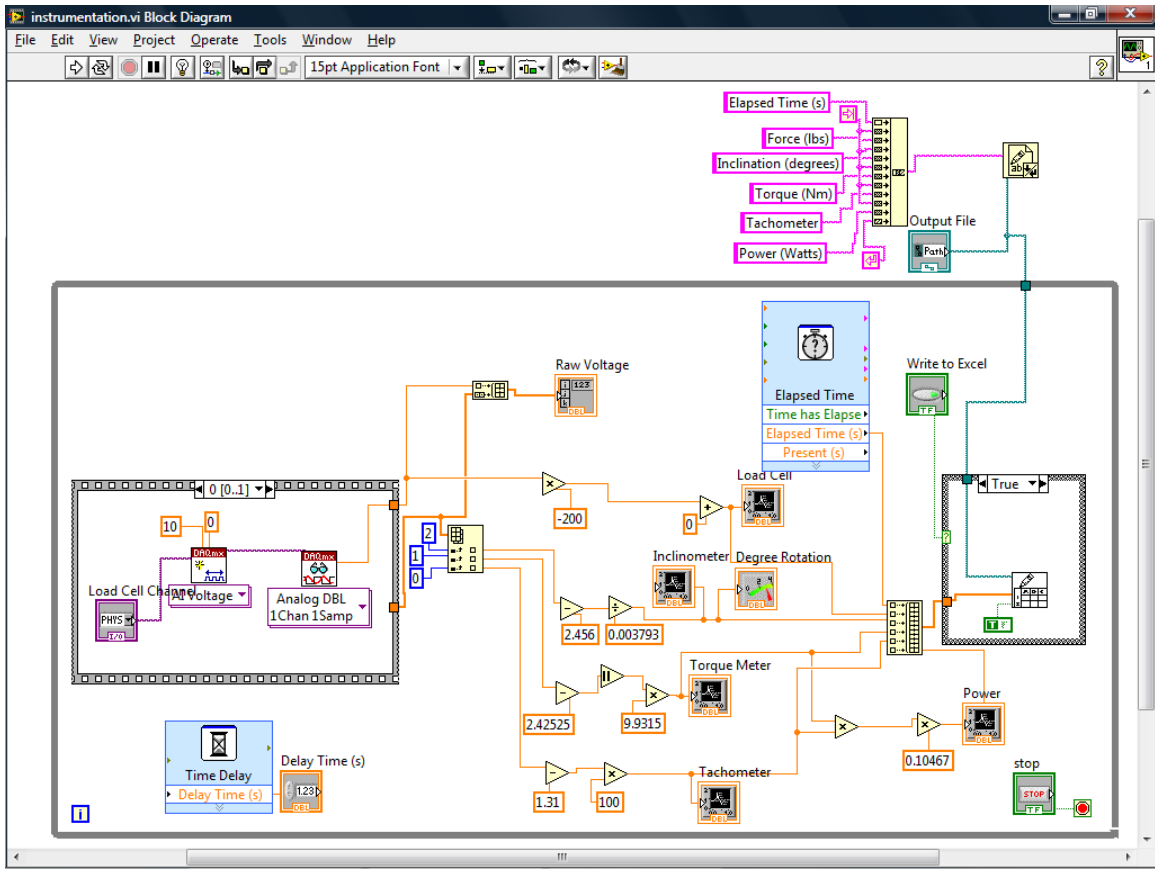


Figure 22: 2009-2010 LabVIEW Block Diagram

There is an orange block labeled power in the bottom right of the block diagram, which corresponds to the plot found in the user interface in Figure 22. Attached to the Power block are the correction factor, torque, and rotational velocity blocks. The data from the Power block is then sent to the excel file in a new column labeled Power (Watts).

10. Lab Testing

Most of the time and effort put forth was on the laboratory testing of our kite power system. The goals of laboratory testing was to evaluate the potential of the system as well as take preliminary field data and apply it to the kite system for safety and to obtain a baseline for future full scale field testing. All laboratory testing was conducted in the aerospace laboratory in the basement of Higgins Labs.

Laboratory testing consisted primarily of using the loading dock in the back of the aerospace lab to test the kite power system using various weighted sandbags simulating the loads that would be produced by the different sized sled kites. The data collected includes torque, angular velocity, arm angle and force of tension on the kite tether.



Figure 23: Kite System Testing Using Sandbags to Simulate Kite Tension

Stringent safety procedures were followed during the laboratory testing process to ensure the safety of everyone. Before a testing session began, the system was moved into place in the loading dock and roped off with caution tape in the area of the moving arms. This zone encompasses the swinging arms and the dropping sandbag. To ensure that the arms are immobilized while team members are in the safety zone setting up the system, a safety brace is incorporated. Safety measures are also taken to allow for safe raising and hanging of the sandbags used for weight during lab testing. Weight in the form of sand bags were raised was raised to about 15' using a chain hoist. Once the sandbag is at the appropriate height, the sandbag is clipped onto a rope connected by a pulley to the kite system arm. The attachment from sandbag to chain hoist is severed and the weight is allowed to drop freely and data is gathered.

The first two testing sessions allowed for our team to become acquainted with the system and understand the mechanics. These sessions were essential to learning the setup and safety rules associated with the system. After our first field session, we were able to use data extracted from LabVIEW using the load cell that our Power Sled 36 kite would provide a force of 35-40 lbs while rising after a stall in winds of 12 mph. Using this data as a guide, a sand bag weighing 40 lbs was used in the first full lab test.

From the results of the previously mentioned lab testing, we are able to obtain important system performance data. The force is applied constantly by the descending sandbag, allowing for recording of time of arm travel. This data becomes important when field testing as the time it takes for the arm to rise and fall is equivalent to the amount of time the kite has to stall and pull to allow for full range of motion. From the lab testing

results in the figure below we were able to determine the average time for the arm to move in its full range of motion with a force of 50 lbs on the system is 8 seconds.

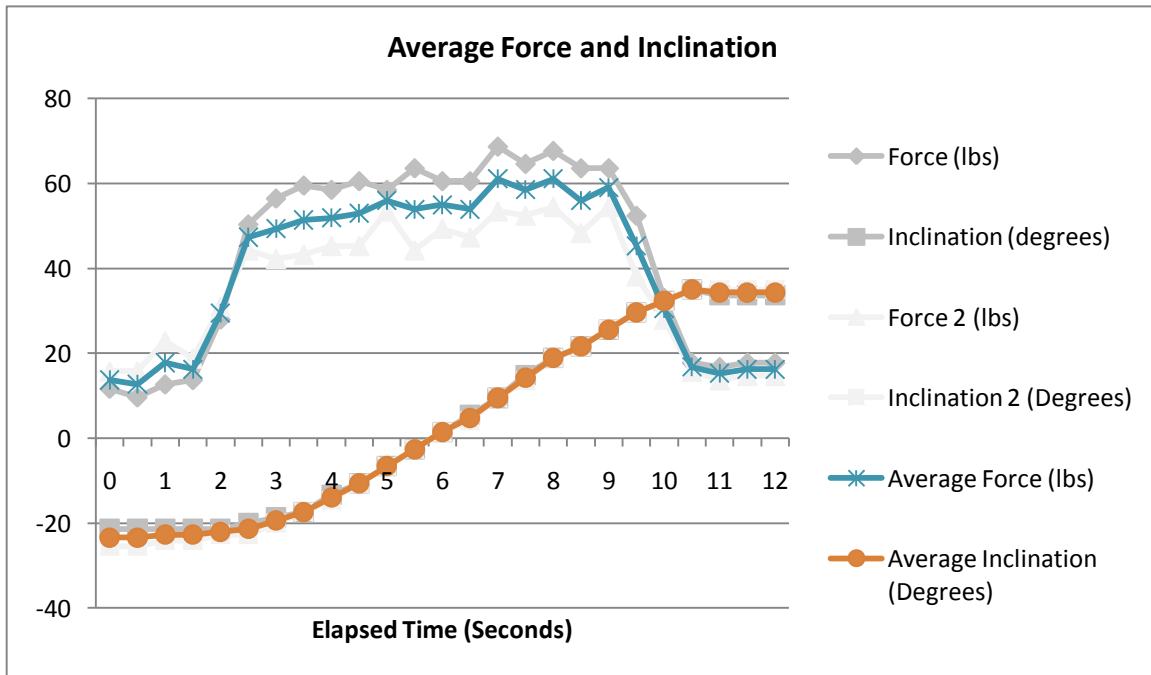


Figure 24: Lab Test-Kite System Weight Drop

As the laboratory testing advanced, individual components of the kite power system were added and removed to see their effect on power generation. Tests were performed with and without the flywheel and dynamometer. The flywheel was originally conceived to keep the generator spinning between the moments of the arms, but through lab testing it was determined it was more detrimental to the system, as it made it too hard to raise the arm attached to the weight/kite. The dynamometer also made the internal belt slip on its flywheel due to increased friction. Due to the laboratory testing we were able to figure out these potential problems before they became larger issues in field-testing. Figure 24 is sample data for the lab testing. Additional data sets were collected and summarized in the Appendix of this report.

Wind Tunnel Testing of Model Kites

The other portion of lab testing concentrated on scaled models of the Power Sled kite and delta wing kite tested in the WPI closed circuit wind tunnel. Models were replicas of Ryan Buckley's wood models from his M.S. directed research project in 2009. The sled kite model was originally built using a 1:5 scale ratio, using dimensions for the full-scale Power Sled 14 sled kite, but due to size constraints, the ratio had to be increased to 1:8.25 scale. The dimensions of these models were measured, modeled in SolidWorks, and printed on the rapid prototyping machine available in Higgins Labs. The root chordlength of the sled kite model was 0.635 feet and the delta kite model was 0.333 feet. Based on scaling factors, the span of the sled kite and delta wing models was 0.833 feet and 0.75 feet respectively. The SolidWorks models are represented in the figures below:

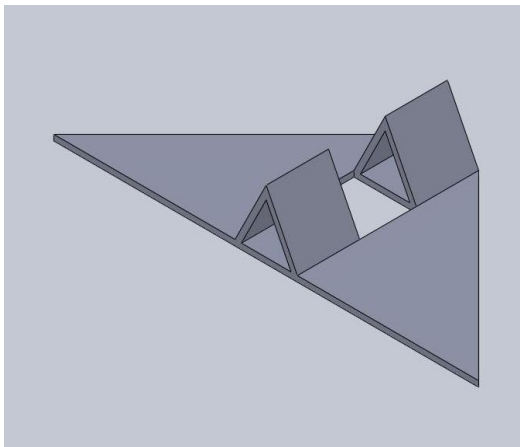


Figure 25: SolidWorks Model Delta Kite

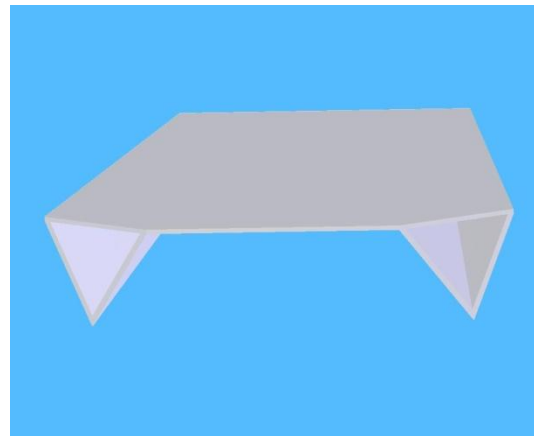


Figure 26: SolidWorks Model Sled Kite

Before wind tunnel testing was conducted on both models, struts attaching the models to the force balance had to be built to raise the models into the center of the Higgins Lab closed circuit wind tunnel. The struts that were previously on the force balance were

too short and therefore the models would have experienced the effects of the walls in the wind tunnel. Before each test the force balance was calibrated to ensure accurate results.

Tests were conducted at a wind tunnel freestream velocity of 72 ft/s to 115.5 ft/s. This corresponded to Reynolds numbers of 301990 and 483180, respectively, based on model root chordlength of 0.635 feet for the test. Given the 1:8.25 scale ratio for the models, this corresponds to a full-scale wind speed for the kites of 8.75 ft/s (5.95 mph) and 13.98 ft/s (9.55 mph) respectively. These wind speeds were lower than originally desired because the restrictions of the rapid prototyping machine forced the models to be smaller than planned. Also, the wind tunnel has the ability to reach speeds greater than 115.5 ft/s, but due to vibrations of the model, the testing could not safely continue past speeds of 115.5 ft/s.

During testing, the lift and drag data at angles of attack from -5 deg to 8 deg were collected. We had to limit our testing to this range due to the observed vibrations in the models. The data was collected and used to create lift coefficient graphs as seen below in Figures 27 and 28. Averaging the lift and drag coefficients over all freestream velocities for each angle of attack led to all the data points found in the graphs below. This data was able to help us more appropriately estimate the expected kite tension line forces of our kite power system.

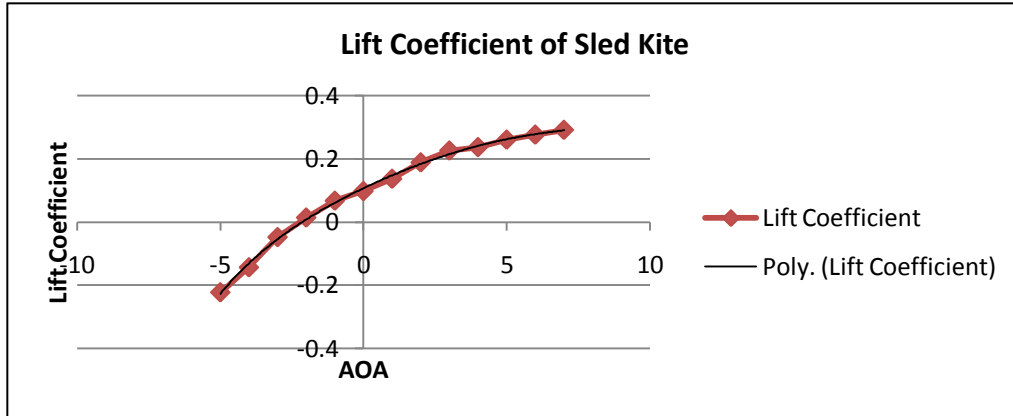


Figure 27: Sled Kite Lift Coefficient

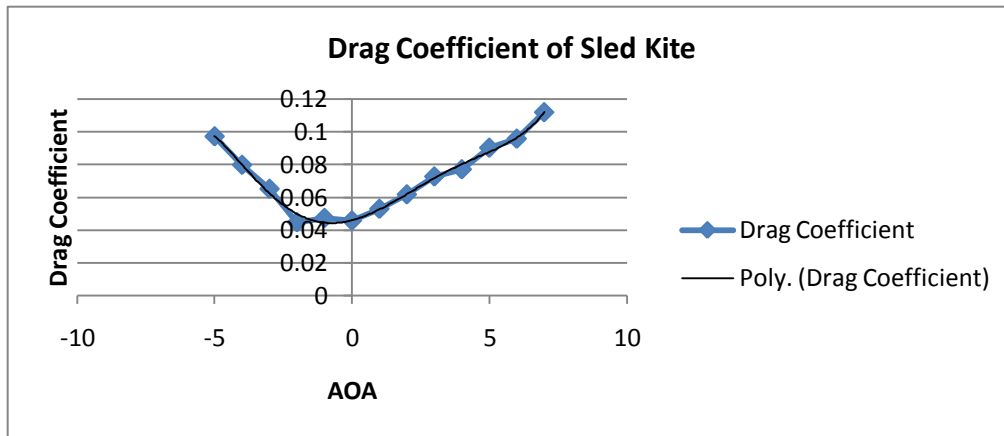


Figure 28: Drag Coefficient of Sled Kite

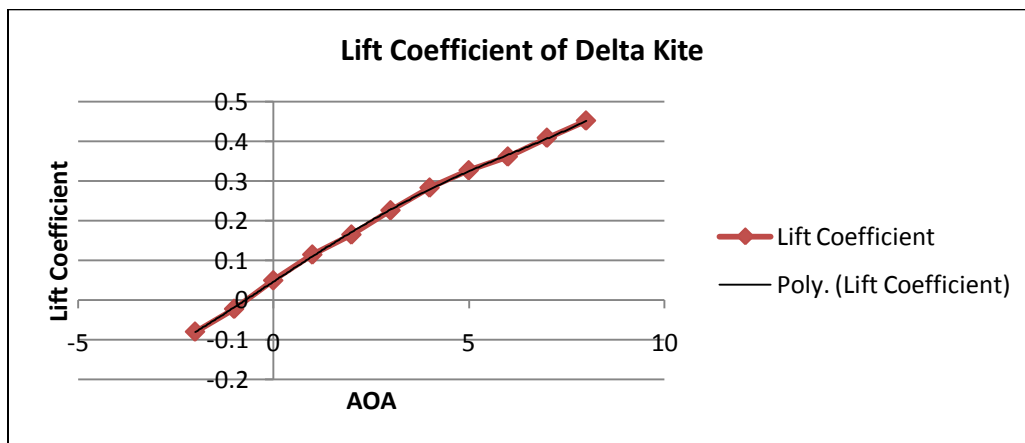


Figure 29: Delta Kite Lift Coefficient

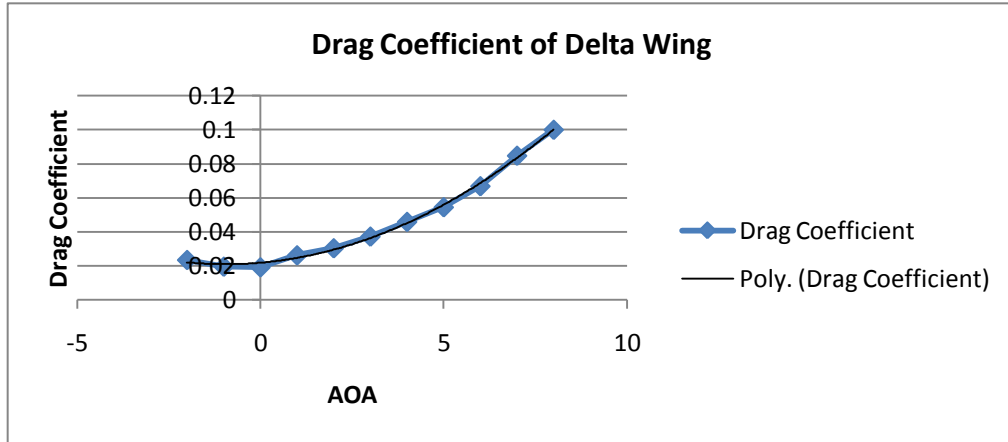


Figure 30: Drag Coefficient of Delta Wing

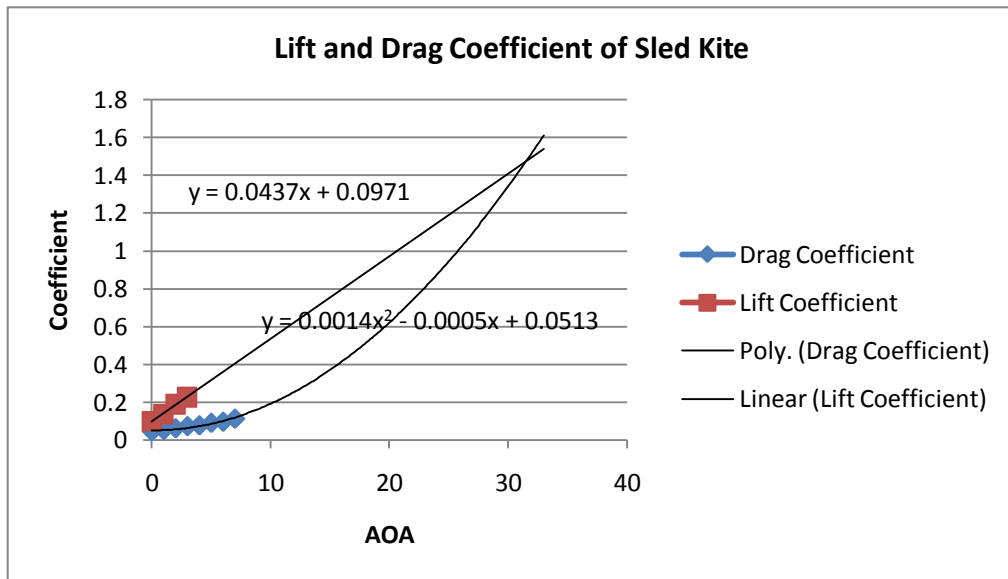


Figure 31: Lift and Drag Coefficient of Sled Kite

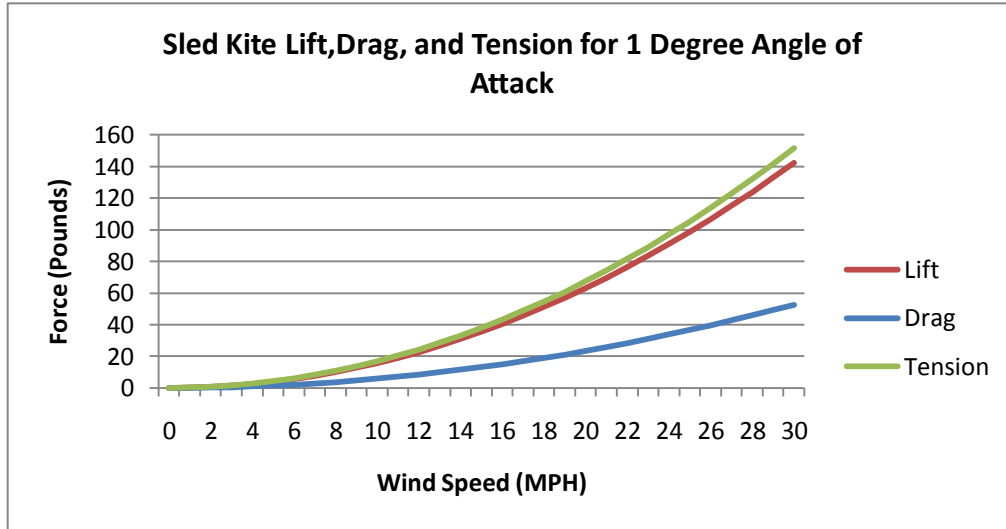


Figure 32: Lift, Drag, and Tension for Sled Kite at 1 Degree AOA

The graphs above each help clarify experimental data and contribute to theoretical data as well. Figure 27 and 28 represent the lift and drag coefficients of the sled kite model. The data generally matched with Ryan Buckley’s hypotheses in his M.S research, but we reached a lower drag and a curved lift coefficient graph. The lower drag was expected because the change in materials from wood to ABS plastic resulted in a more aerodynamic model. The lift coefficient curve should have been linear, but this is explained from the vibrations at both higher wind speeds and higher angles of attack. At lower angles of attack, from 0 to 4 degrees, the line is highly linear and therefore those data points were used to predict lift coefficients at higher degrees.

Figure 31 shows the expected results if the trendline of the drag and lift coefficients were extended to an angle of attack of about 33 degrees. This figure assumes that the lift coefficient is linear and that the drag coefficient is a second order polynomial. Based on these assumptions, a successful stall should occur at about an angle of attack of 31 degrees because that is where the drag and lift coefficients intersect. Though not deduced

experimentally, this data is reasonable because the kite does not require a high angle of attack to stall.

Finally, the tension in the kite tether can be established using the lift and drag coefficients. Using data in the field, such as an expected tensile force of 15 pounds at a wind speed of 10 mph, forces can be assumed for a vast array of wind speeds. Using the lift coefficient found in the wind tunnel, dimensions of the Power Sled 14 Kite, and the wind speeds found experimentally, the lift and drag versus angle of attack can be approximated. Based on that data, an expected angle of attack can be chosen that matches the experimental tensile forces to the forces found from the coefficients. Therefore, the kite flies at an angle of attack approximately equal to one degree. Based on a one-degree angle of attack, the lift, drag, and tensile forces are plotted in Figure 32 for a number of wind speeds. Based on field testing data, the wind speeds are generally between 10 and 20 mph. Therefore, the expected tensile force in the tether of the Power Sled 14 Kite is between 15 and 65 pounds force. If we assume that the sled kite model tested in the wind tunnel has the same coefficients for all three sled kite sizes (this is not necessarily the case, the larger sled kites have different geometries), then further tensile forces can be deduced. The Power Sled 36 Kite will have tensile forces between 40 and 160 pounds, and the Power Sled 81 Kite will have tensile forces between 90 and 375 pounds based on the same wind speeds and coefficients used for the Power Sled 14 Kite.

11. Field Testing

This year one of the main focuses of the group was field testing with the newest sled kites as well as the entire system. The goal was to evaluate and compare the results gained in lab testing to real world conditions. Most of the field testing was completed at a public beach in Seabrook, New Hampshire and because of our reliance on weather conditions, most of the testing was done during the fall and spring months.

The majority of time spent in the field was devoted to testing the feasibility of a sled kite instead the originally tested kiteboarding kites as well as gathering data using the load cell. Throughout the course of the year, we tested three sled kites of varying sizes, whose dimensions are shown in Figures 33, 34, and 35. Because of their stability, we determined a sled kite was a better choice to power the system. We were able to measure the forces generated and also gather data when the trailing edges of the kite were pulled to stall the kite. This is the first time we know of trailing edge lines have been added to a sled kite in order to allow for stalling and unstalling. After testing in Seabrook multiple times and with different kites, we saw how easily sled kites can be stalled in a controllable, stable fashion by pulling on these trailing edge lines. After preparation in the lab, the entire kite system was taken to the field for the first time in two years in April 2010 and tested while attached to the medium-sized sled kite, the Power Sled 36.


Size (w x l)	63 x 40 in. / 160 x 102 cm.	
Wind Range	6 ~ 20 mph	
Fabric	Ripstop Nylon	
Packaging	Drogue Chute Bag	
Line	Includes 500 ft. 90 lb. Test Line on Yo-Yo Winder	

Figure 33: Power Sled 14 (<http://www.premierkites.com/collections/pdf/Sleds.pdf>)

Size (w x l)	127 x 59 in. / 323 x 150 cm.
Wind Range	5 ~ 20 mph
Fabric	Ripstop Nylon
Packaging	Drogue Chute Bag
Line	Recommended 500 lb. Test Line



Figure 34: Jumbo Power Sled 36 (<http://www.premierkites.com/collections/pdf/Sleds.pdf>)

Size (w x l)	178 x 83 in. / 452 x 210 cm.
Wind Range	5 ~ 20 mph
Fabric	Ripstop Nylon
Packaging	Drogue Chute Bag
Line	Recommended 1000 lb. Test Line

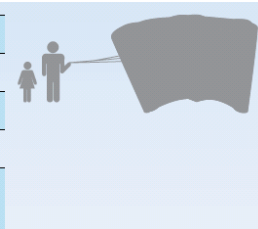


Figure 35: Mega Power Sled 81 (<http://www.premierkites.com/collections/pdf/Sleds.pdf>)

During our first test in Seabrook in fall 2009, the need for a redesigned load cell configuration became apparent when the forces the load cell read were not reliable, even after the load cell was recalibrated. When in the air, the sled kite flew at angles between 30 and 60 degrees and because the line did not pull straight on the load cell, the forces measured were not accurate. As already described in the instrumentation section, a new design allowing for the free movement of the load cell was created and fabricated. When tested again in the field with this new design, the load cell began reading more accurate measurements of force.

Most of the tests completed at Seabrook were done using the Power Sled 36 kite which had been previously purchased but never flown in the field. When first testing this kite, we attached only the main lines to the truck hitch to monitor the movement of the kite under current wind conditions. Once it was seen how stable the kite became in the air, we then attached trailing edge lines to both the kite and steering mechanism previously used

with the kiteboarding kite. This mechanism allowed the kite to be stalled while in the air by pulling the slider downward, shown below.



Figure 36: Kite Stalling Mechanism

Once stalled, the kite moves downward until the controller releases the sliding bar pulling down the trailing edge lines. When released the kite reopens and returns to its normal steady state. Data taken in the field proved the most force is generated at the instant the kite is released from stall and begins to steady. With this medium kite, the average forces we read during normal and stalling stages were about 15lbs during flight and 35lbs when the trailing edge lines are initially released. The figure below shows the

data gathered for multiple stalls during one of the Seabrook testing days. The black line corresponds to the average of all data taken that day and the quick increase in the slope of the line matches up with the time immediately after the kite is released from stall and then slowly gains altitude again.

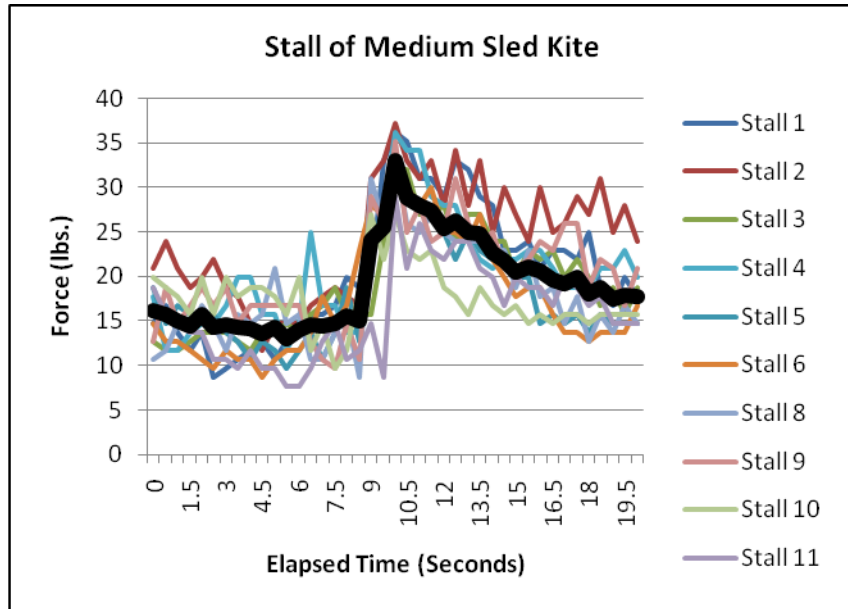


Figure 37: Stall of PowerSled 36

In order to achieve the forces needed to realistically move the arm of the system, the group purchased a larger kite, the Power Sled 81, to test in the field and compare with the forces generated by the medium kite. When tested at Seabrook under higher wind speeds, it was able to produce forces roughly double those of the PowerSled 36. This larger kite had an average force of 40lbs on the load cell when flying steadily. When stalled, the force decreased to 30lbs, then jumped to 80lbs when first released.

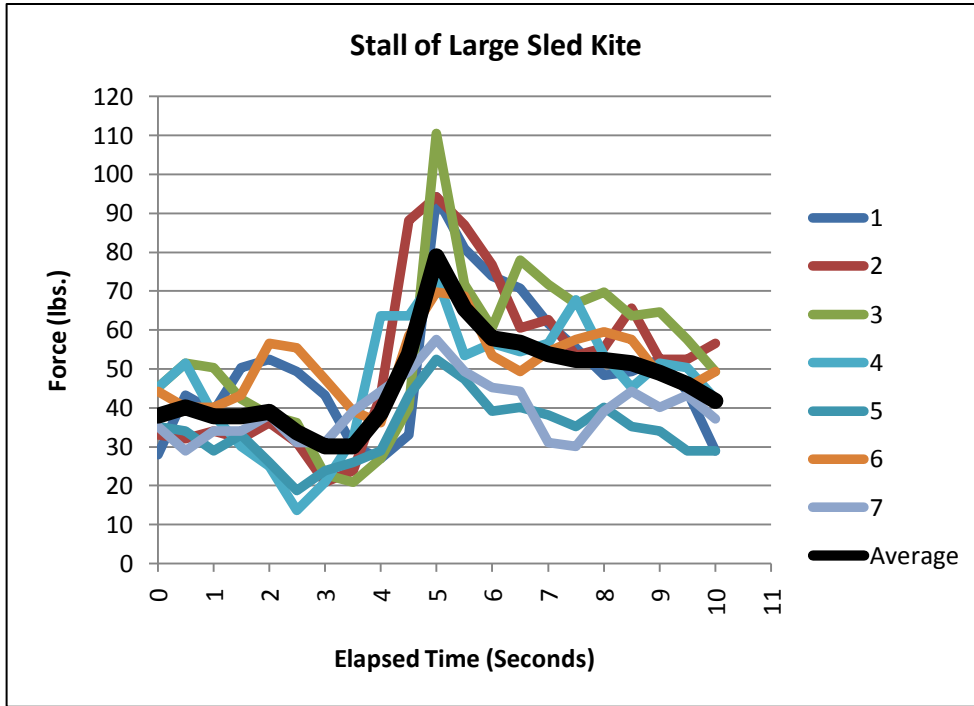


Figure 38: Stall of PowerSled 81

After thorough testing in the lab and with the medium kite, the group also took the A-frame structure to beach to test the entire system in early April 2010. The system was transported to the beach and once there, secured in the sand using four arrowhead sand anchors. Since we wanted to take every safety precaution possible, the arm was also secured to the sand using an anchor and tie-down until the kite was stalled and the movement of the medium-kite could be monitored. After manually stalling the kite using line attached to the sliding mechanism and run to the back of the system, the tie-downs were loosened, allowing for some movement of the arm. Small amounts of weight were also added to the back end of the arm to help the movement of the arm when stalling.

The first full kite system test was a success, the kite stalled, the rocking arm moved, and accurate data was gathered throughout the process. The tests began with the rocking arm securely tied down to ensure safety. Once a successful stall of the medium sled kite

resulted in controlled motion of the rocking arm, the safety tether was extended, allowing for about 20 degrees of motion from the lowest point.



Figure 39: Full System Test with Kite



Figure 40: Overview of System

Figures 39 and 40 above show the system in its most downward position. The rocking arm is at its lowest point before the force from the kite pulls the arm up to the controlled position. Following the initial tests of the arm movement, the laptop was setup to begin recording data from the four sensors on the system.

The data gathered from the sensors during the first full kite system test proved to be useful. The sensors gathered the tension in the kite tether, the inclination of the rocking arm, and the torque and rotations per minute of the driveshaft. The data was gathered in an excel file and is shown in the following figures.

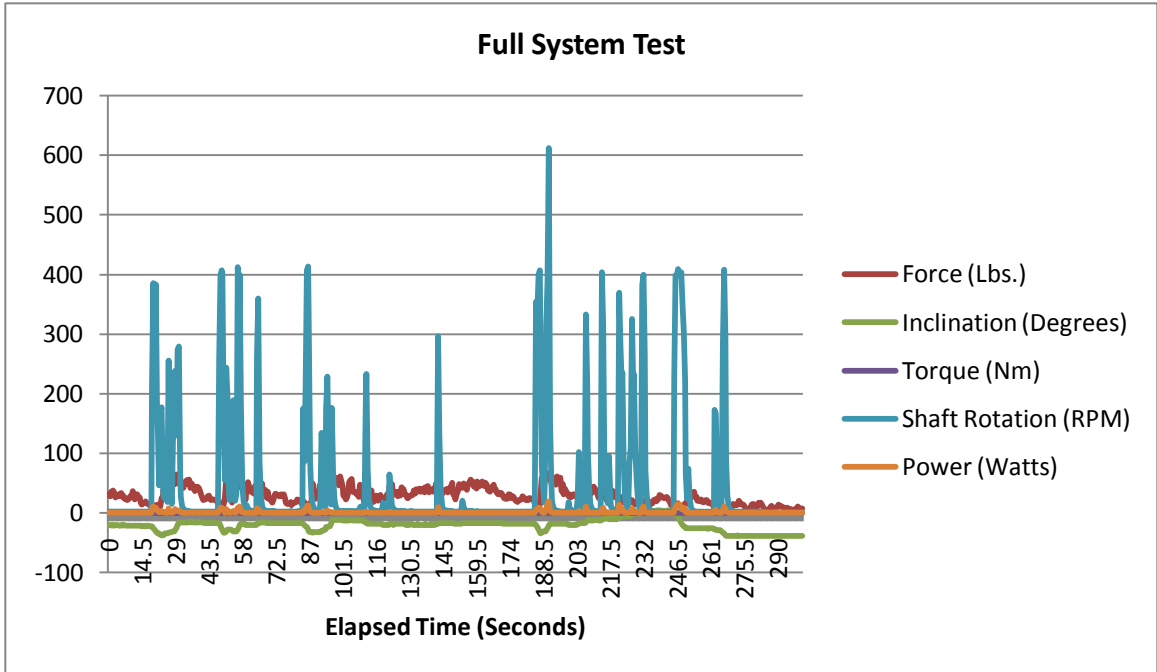


Figure 41: Full Data Set from Kite System Test

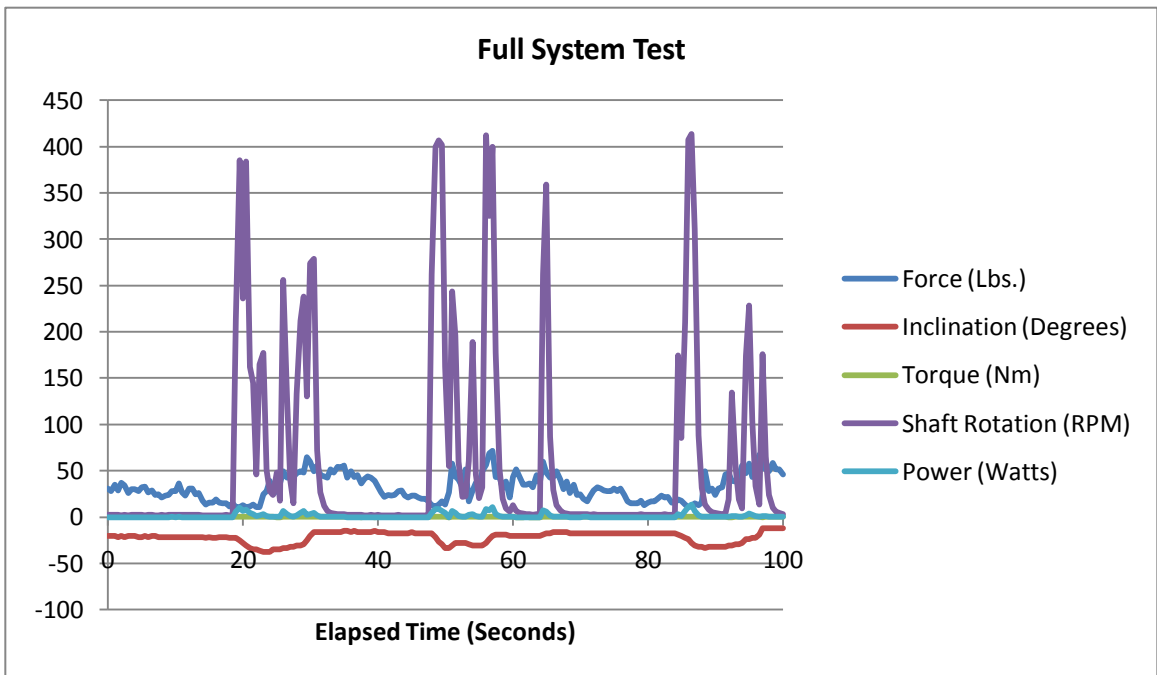


Figure 42: Kite Stalls from Kite System Test

Figure 41 represents the full data gathered during the kite system testing. Figure 42 is the data gathered from the first 100 seconds of testing. Three successful cycles of the rocking arm were conducted and shown in Figure 42. The stall of the kite begins at about

the 15-second mark and takes about 5 seconds to release enough tension to begin moving the rocking the arm. The rocking arm falls at the 20-second mark when the tether line tension from the kite is at the lowest point. Once the rocking arm reaches its lowest point, -37.5 degrees, the kite is unstalled manually by the person releasing the kite control bar and the tether line tension rapidly increases to about 60 pounds force. The arm reaches its maximum positive angle (restricted by the safety chain on the arm) about five seconds after the kite is released from stall. As long as the arm is in motion, the drive shaft rotates due to the two-belt system attached to both sides of the rocking arm. Interestingly, the kite system generates the highest rotations per minute when the rocking arm is descending rather than ascending.

This first trial was a “no load” trial. The drive shaft was left to freely rotate without any applied load, such as a dynamometer or generator. Therefore the torque generated during the test varied between low values of zero Newton-meters and 0.3 Newton-meters. Once the generator is attached to the drive shaft the torque should increase and the rotations per minute should decrease. The calculated power, due to the low torque, reached a maximum value of 15 watts. If the torque were to increase to about 1.5 Newton-meters and the rotations per minute decreased to about 250, then the power would increase to about 40 watts. Also, if the system were allowed a full range of motion then both the rotation of the drive shaft and the torque would increase due to the acceleration of gravity on the rocking arm.

12. Conclusions

By replacing the previously used kiteboarding kites with a sled kite, a great deal of progress was made in creating a system that could function autonomously. While the current system still requires an operator, the kite remains stable in the air on its own far longer than the previously used kiteboarding kite. Redesigning the sliding mechanism on the rocking arm was a primary goal of this project, and resulted in a mechanism with about half the weight of the previously used concept. With this weight reduction, the team was also able to increase the travel on the slider, making it easier to consistently stall the kite. Stalling the kite properly is integral to the function of the kite power system, and this new mechanism proved a competent replacement. These improvements increased the feasibility and functionality of the system, bringing it closer to functioning at its theorized level.

Noticing a great deal of resistance when manually moving the rocking arm, the team also moved forward with some redesign of the drive shaft mechanism that translates the mechanical energy produced from the kite to electrical energy. The main change made was that the flywheel included in the initial design was removed, further improving the ability of the system to function properly. The flywheel was originally intended to store energy as the rocking arm moved downward, but with last year's addition of a second nylon strap to one end of the rocking arm to produce power during the kite descent, the flywheel became erroneous, and so was removed. The locking mechanism that held the rocking arm stationary when not in use was also redesigned. The original design was a U shaped lock that failed on the team on one of our first days of lab testing. To account for this, the team

cut two very thick pieces of angle iron into the appropriate shape to rest on the system, under the rocking arm, eliminating any future possibility of a lock failure.

The data acquisition tool was also streamlined to be used in the field. By configuring the components to be powered by USB, teams working on this project are now able to take the data acquisition device with them to the field and observe the data being collected in real time. With this streamlined DAC also came a redesign of the load cell used to measure the forces produced by the Kite. Originally, the load cell could only measure forces in the z (upward) direction, and it now resides in a casing that moved with the kite, allowing accurate measurement of the forces produced in the x, y, and z directions.

Extensive lab testing was conducted over the course of the project, with large sandbags on a pulley system being used to simulate a load on the system. By running the system through many full cycles, and the use of the improved DAC, the team was able to collect a great deal of data that helped to support the feasibility of the system. Two kite models (for a sled and a delta wing kite) were created on the rapid prototyping machine for use in wind tunnel testing. These models were tested at length in a wind tunnel, and from these tests accurate lift coefficients were produced for all of these models.

In synopsis, this year's team has greatly improved the WPI kite power system's functionality and usability. With the improved stability offered from the sliding mechanism and kite, the system is a few steps closer to permanent installation in a developing nation.

13. Future Work

Even though we achieved the original goals of the project, such as testing and improving the system, there is still work to be done in the future. The final field test of the entire kite system resulted in certain problems that need to be addressed.

First and foremost, the rocking arm needs to be balanced in order to achieve optimal movement. The end of the rocking arm with the slider requires more weight in order to lower the rocking arm when the kite is stalled, but the sliding mechanism cannot weigh too much so that the kite is unable to pull the rocking arm up during kite ascent. Unfortunately, the sliding mechanism also needs to have enough weight to ensure it overcomes the friction in the guide rods and therefore requires more weight than is required for arm movement. Therefore, a variable weight system is recommended that would change the weight on the ends of the rocking arm depending on the inclination. When the kite is stalled there should be additional weight on the opposite end of the rotating arm, but when the kite is unstalled the weight should be moved closer to the center of the rotating arm to decrease the moment and therefore nullify the added weight. With a new system, the rotating arm should be able to move more consistently during kite ascent and descent.

The first field test of the entire system did not include a load on the drive shaft. Therefore the measured instantaneous power was lower than should occur during actual system operation. Further field and lab tests need to be conducted with a generator and load attached to the system. The forces needed to overcome a load on the driveshaft will probably change and therefore lab tests are necessary to optimize the weights on the

rocking arm prior to field-testing. With the addition of the generator, the calculated instantaneous power can be compared to power produced from the generator.

The large sled kite should also be tested on the full system. The medium sled kite achieved forces up to seventy pounds, but the large sled kite should be able to achieve higher applied forces, resulting in more consistent rocking arm motion and ultimately more power produced.

Finally, the ultimate goal of the project is to implement the system in a coastal, African nation such as Namibia. There needs to be further research done to ensure that the kite system can be setup in a small village to bring cheap electricity to those who need it most. Different construction materials, such as steel replacing the wood structure of the system might be necessary to increase the usable lifespan of the system. Compatibility between current electricity systems in Namibia and the kite system should be researched. Finally, some sort of re-launch system should be developed for the kite for when the wind velocity reduces to low levels, and the kite cannot maintain altitude. This is particularly important since system capacity, e.g. the percent time that a wind power system is producing usable power, is an important consideration in wind power economics.

14. Reference List

- ¹ REN21. 2009. "Renewables Global Status Report: 2009 Update" (Paris: REN21 Secretariat).
- ² Alex, L., Eric D., Luke F., Scott Gary., (2009). *Design of a Data Acquisition System for a Kite Power Demonstrator*. MQP Project #DJO-0109, Worcester Polytechnic Institute, Department of Aerospace Engineering, Worcester.
- ³ Postock, G., "The Aeropleustic Art or Navigation in the Air by the use of Kites, or Buoyant Sails", London, 1827
- ⁴ . Loyd, M.L., 1980, "Crosswind Kite Power", *J. Energy*, 4(3), pp 106-111.
- ⁵ Goela, J.S. "Wind Energy Conversion Through Kites." January 1983.
Indian Institute of Technology Kanpur
- ⁶ Goela, J. S., 1983, "Project Report II on Wind Energy Conversion Through Kites", DST Project Report No. DST/ME(JSG)/81-84/26/2, IIT Kanpur.
- ⁷ Goela, J.S. "Wind Energy Conversion Through Kites." January 1983.
Indian Institute of Technology Kanpur
- ⁸ Lang et al., "Electrical Power Generation Using Kites", 2005
- ⁹ Martinelli, N. (2006, October 10). *Generating Power From Kites*. Retrieved January 3, 2009, from Wired Magazine Online: <http://www.wired.com/science/discoveries/news/2006/10/71908>
- ¹⁰ Highest Wind LLC, "Highest Wind Info Sheet", 2009. Online: <http://highestwind.com>
- ¹¹ Blouin, M., Isabella, B., & Rodden, J. (2007). *Wind Power from Kites*. MQP Project #DJO-0107, Worcester Polytechnic Institute, Department of Aerospace Engineering, Worcester.
- ¹² Buckley, R., Colschén C., DeCuir M., Simone N., Lovejoy E., Hurgin M., (2008). *Design of a One Kilowatt Scale Kite Power System*. MQP Project #DJO-0308, Worcester Polytechnic Institute, Department of Aerospace Engineering, Worcester.

15. Appendix

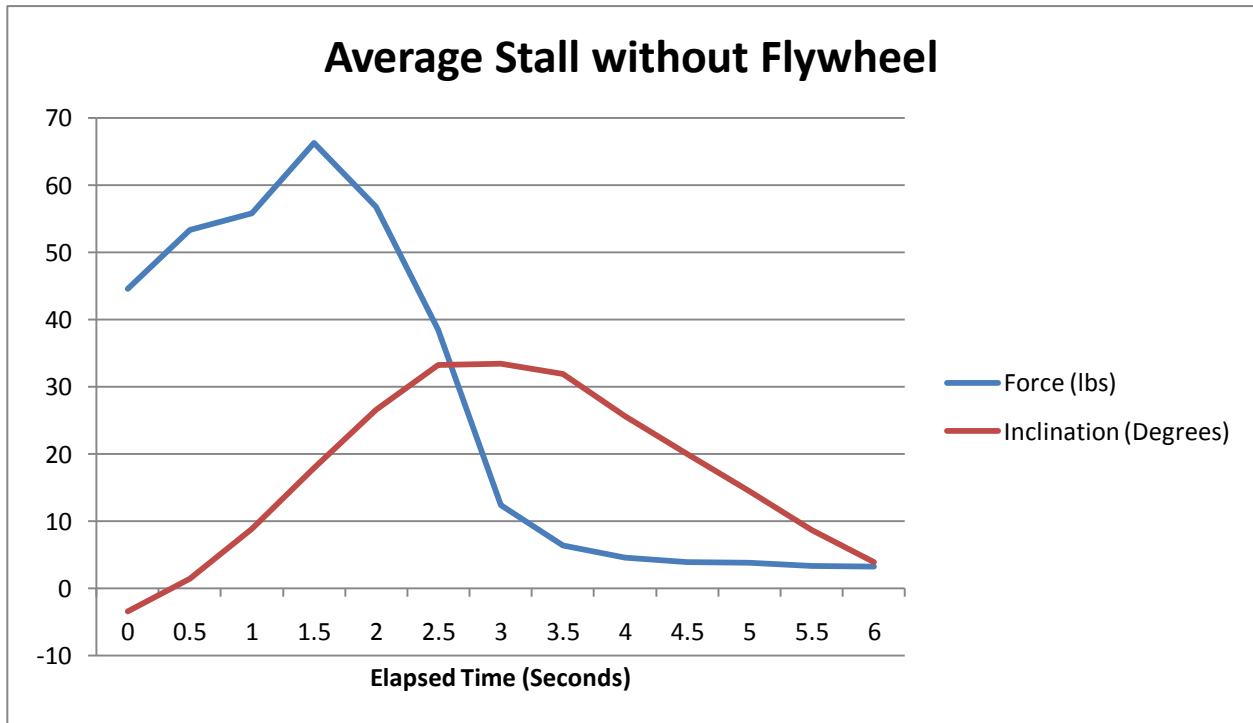


Figure 43: Test One without Flywheel

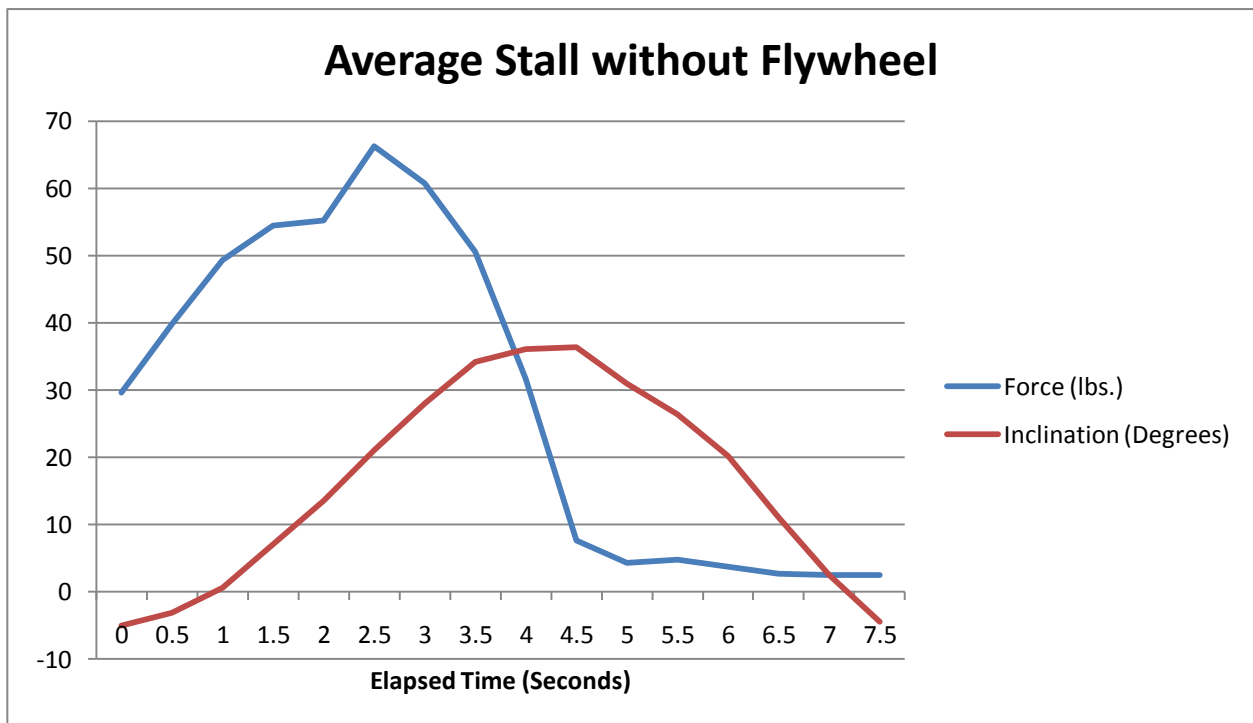


Figure 44: Test Two without Flywheel

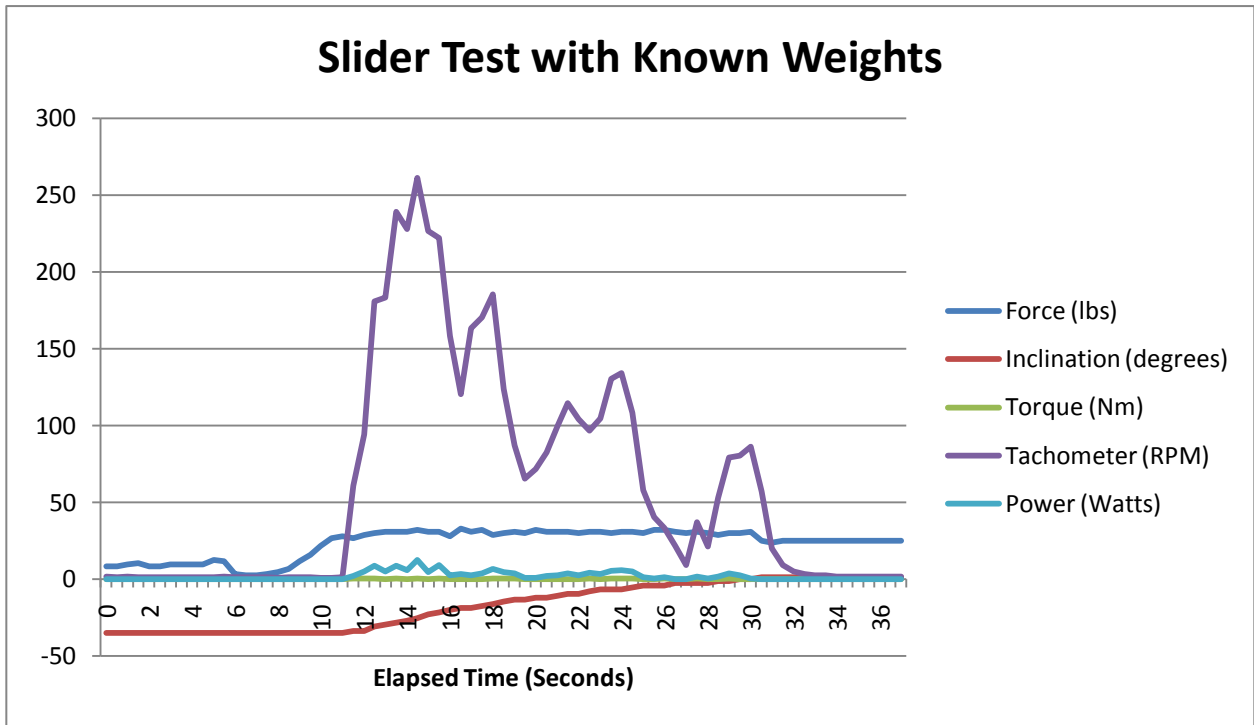


Figure 45: Test One with Sliding Mechanism

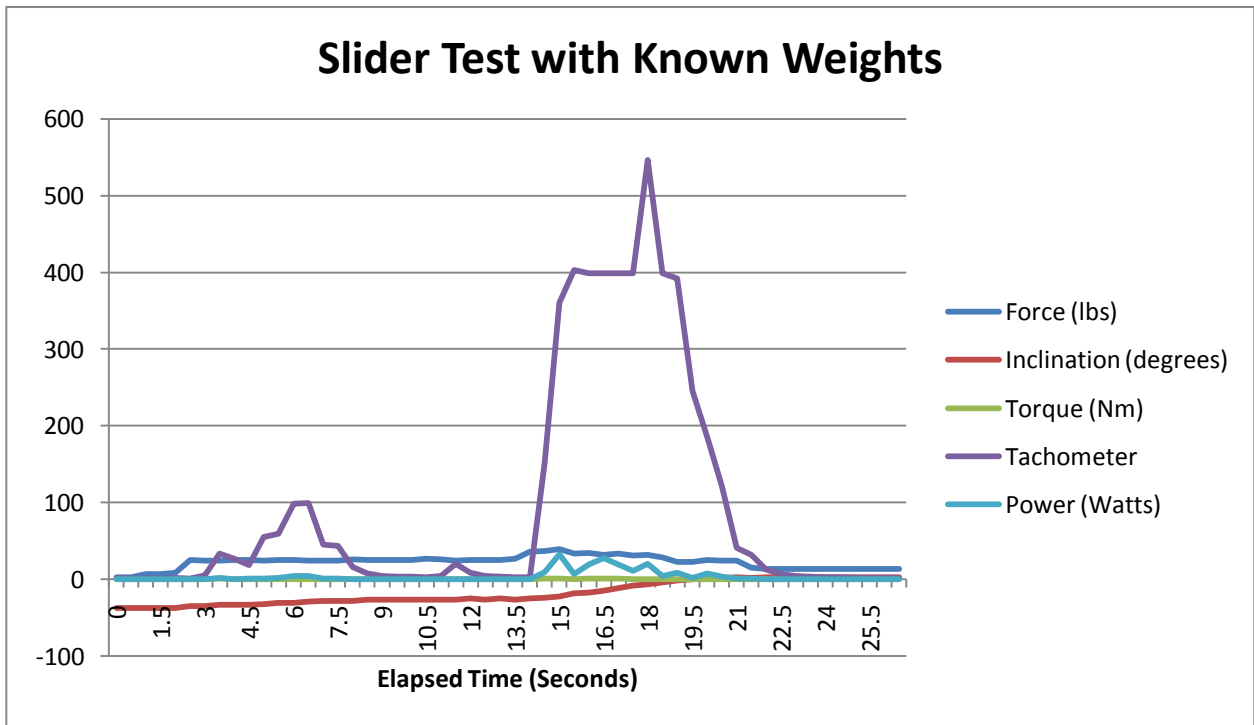


Figure 46: Test Two with Sliding Mechanism